Journal of Hydrology: Regional Studies 66 (2026) 103692

Contents lists available at ScienceDirect

Journal of Hydrology: Regional Studies

journal homepage: www.elsevier.com/locate/ejrh

Application of the water accounting plus (WA+) framework for the assessment of water availability and consumption in the Zambezi River Basin (ZRB)

Micheal Katongo Phiri [a,*], Kawawa Banda [a], Mansoor Leh [b], Naga Velpuri [b], Primrose Tinonetsana [b]

[a] University of Zambia – Integrated Water Resources Management Centre, Department of Geology, School of Mines, Lusaka, Zambia
[b] International Water Management Institute, Colombo, Sri Lanka

ARTICLE INFO

Keywords:
Zambezi River Basin
Water Accounting Plus
Water consumption
Water availability
Remote sensing
Evapotranspiration
Transboundary water management

ABSTRACT

Study region: The Zambezi River Basin (ZRB) is a large transboundary basin in south-central Africa shared by eight countries. It provides vital water resources for hydropower, agriculture, ecosystems, and human use across the region.
Study focus: The remote sensing-based Water Accounting Plus (WA+) framework was applied to the ZRB from 2003 to 2023 to quantify its water balance. The WA + methodology was used to overcome sparse ground data by leveraging satellite-derived datasets such as precipitation (P), actual evapotranspiration (ET_a) and land cover and use (LULC).
New hydrological insights for the region: The WA + water balance for the ZRB reveals that P (1280.5 km^3/year) is the dominant inflow, while ET_a (1095.6 km^3/year) constitutes 85.5% of the gross inflow. This leaves a long-term mean *surface water yield* (P–ET_a) of 184.9 km^3 /year. A substantial portion of the inflow (115.9 km^3/year) is lost to storage, suggesting significant basin-scale water-storage potential. The exploitable water averages 106.6 km^3 /year, of which 19.9 km^3 /year is reserved outflow and 0.2 km^3 /year is non-utilisable outflow; thus, about 86.4 km^3 /year remains available for use. Currently, 44.5 km^3 /year is utilised flow, leaving 42.0 km^3 /year that is still undeveloped. Overall, the basin sustains a net-positive water balance, though water availability declined over the study period, coinciding with a general downward tendency in P and elevated ET_a in recent years; however, the basin-scale trends in P and ET_a were not statistically significant.

1. Introduction

The Zambezi River Basin (ZRB) is one of the most important transboundary river systems in Africa. Extending across eight riparian states in south-central Africa, it supports hydropower generation, agriculture, fisheries, wetlands, tourism, and domestic water supply, while sustaining the livelihoods of more than 30 million people across the region (Beilfuss, 2012; World Bank, 2010). The basin is also hydrologically and ecologically significant, containing major wetlands, floodplains, and large regulated reservoirs that underpin both ecosystem functioning and regional economic development. At the same time, water resources management in the ZRB is complicated

* Corresponding author.
E-mail address: kmphiri@nrsc.org.zm (M.K. Phiri).

https://doi.org/10.1016/j.ejrh.2026.103692
Received 7 July 2025; Received in revised form 16 June 2026; Accepted 26 June 2026
Available online 1 July 2026
2214-5818/© 2026 The Authors. Published by Elsevier B.V. This is an open access article under the CC BY license (http://creativecommons.org/licenses/by/4.0/).

by strong spatial and temporal variability in water availability and by recurrent droughts and floods (Beilfuss, 2012; Hughes and Farinosi, 2020; Hulsman et al., 2021). Earlier work has also highlighted trade-offs among hydropower production, downstream ecosystem requirements, and other water uses, together with operational pressures associated with major reservoirs such as Kariba and Cahora Bassa (Beilfuss, 2012). These pressures are further amplified by the transboundary nature of the ZRB, which makes coordinated planning, allocation, and governance across riparian states both necessary and challenging.

These conditions create a strong need for basin-wide, transparent, and policy-relevant assessments of water availability, depletion, and use. Water accounting provides one such framework by systematically tracing the status and trends in water supply, demand, distribution, accessibility and use within a given domain over time (FAO, 2012; Batchelor et al., 2016). In doing so, it can support improved decision-making and the implementation of Integrated Water Resources Management (IWRM). However, comprehensive implementation of water accounting in poorly gauged basins, such as the ZRB, remains challenging due to sparse hydro-meteorological observations and limited water-use data. Conventional frameworks such as the System of Environmental-Economic Accounting for Water (SEEAW) (United Nations, 2012) are data-intensive and are therefore difficult to apply comprehensively in data-sparse basins.

The Water Accounting Plus (WA+) framework has emerged as a viable alternative for such basins. WA + is a remote sensing-based framework that integrates consistently collected spatial datasets to estimate water balance components. It was developed as a modified version of the International Water Management Institute water accounting (IWMI WA) framework (Bastiaanssen, 2009; Karimi et al., 2013a). As such, the WA + framework follows the principles of the IWMI WA and tracks water depletion rather than withdrawals. It explicitly quantifies actual evapotranspiration (ET_a) and relates outflows to net inflows, thereby avoiding errors associated with untracked return flows (Karimi et al., 2013a). WA + also recognises the influence of land cover/use (LULC) on the water cycle and tracks water depletion across Water Accounting Land Use (WALU) classes (Bastiaanssen et al., 2015). Remote sensing has been shown to estimate key water-balance components with relatively high accuracy, making it suitable for basin-scale water accounting (Karimi and Bastiaanssen, 2015). Accordingly, WA + has been applied in data-sparse river basins such as the Indus, Ca, Volta and Lake Tana basins (Karimi et al., 2013b; Bastiaanssen et al., 2015; Dembélé, et al., 2023; Owusu, et al., 2025; Mekonnen, et al., 2026).

Recent studies have examined the ZRB from hydrological, drought, and climate-change perspectives, including basin-wide assessments of development and climate variability impacts on water resources (Hughes and Farinosi, 2020), satellite-based analyses of drought conditions in the basin upstream of Kariba (Hulsman et al., 2021), and climate-change impacts on streamflow in Zambezi sub-basins such as the Kabompo (Ndhlovu and Woyessa, 2021). However, these studies do not provide a basin-wide water accounting assessment of water availability, depletion, and consumption for the entire transboundary basin. In particular, they do not apply the

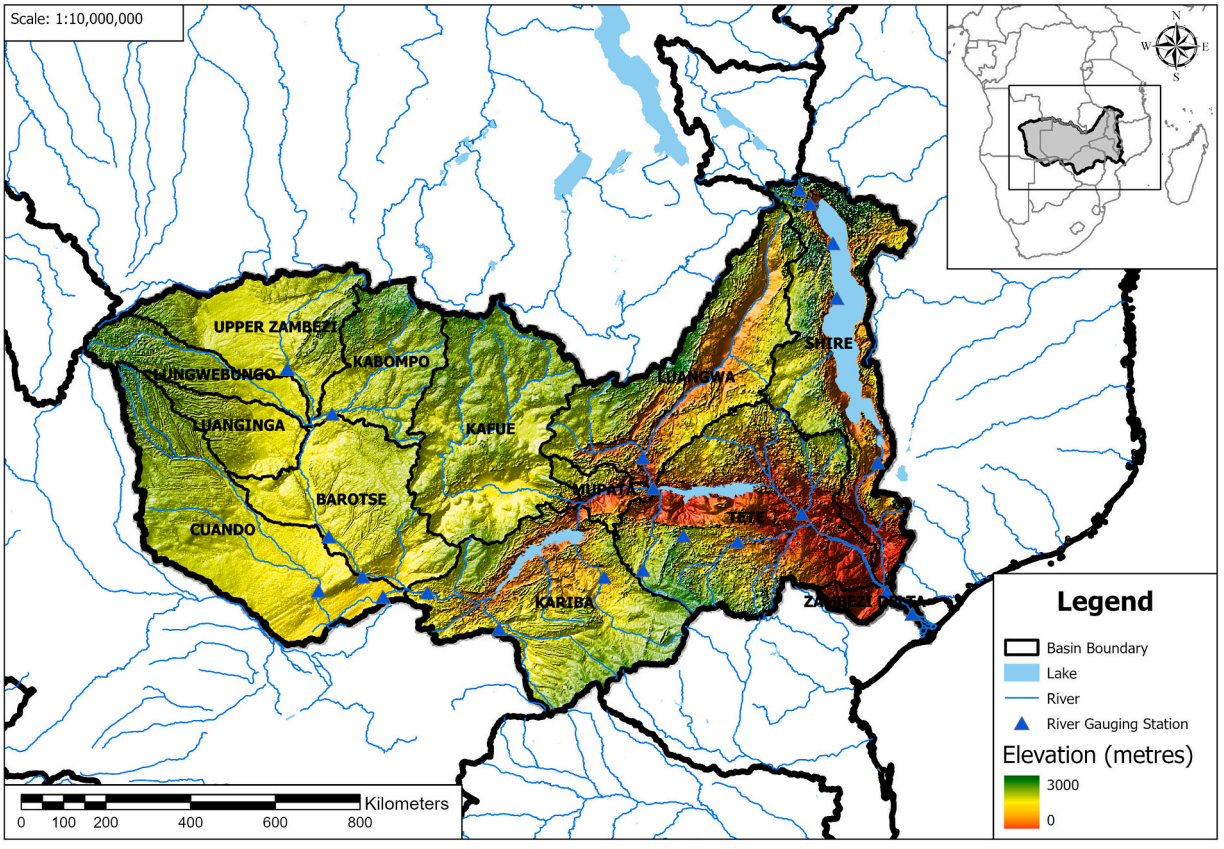


Fig. 1. The Zambezi River Basin in south-central Africa.

WA + framework to generate a spatially distributed, basin-wide account linked to land use.

Previous water-accounting efforts relevant to the region have largely been undertaken at the national scale using SEEAW/SEEA-Water approaches rather than as a single transboundary basin-wide account (Republic of Botswana, 2016; Republic of Zambia, 2020). The present study addresses this gap by applying the WA + framework to the entire ZRB from 2003 to 2023. To the best of our knowledge, this is the first peer-reviewed basin-wide application of the WA + framework to the entire ZRB. In doing so, it goes beyond previous basin studies by providing a spatially distributed account of water availability, depletion and consumption, with explicit attribution of water use to land and water-use classes through the WALU framework. The study further establishes a consistent multi-year account for 2003–2023, enabling examination of interannual variability, recent hydroclimatic anomalies, and broader basin-scale dynamics over two decades. More broadly, the approach offers a transparent and replicable methodology for water accounting in other data-sparse transboundary basins, where comparable evidence is needed to support basin planning, allocation decisions, and cooperative governance. The use of WA + in the present study is supported by prior applications demonstrating the consistency of remote-sensing-based water accounting outputs. For instance, a WA + application in the Awash Basin, Ethiopia, found that key WA + parameters and performance indicators exhibited coefficients of variation below 20% across multiple years (Karimi, et al., 2015), indicating relatively stable outputs. This strengthens the case for applying WA + in the ZRB.

Against this background, the aim of this study was to apply the WA + framework to the ZRB to assess water availability and consumption for the period 2003–2023. Specifically, the study sought to: (i) quantify the main basin-scale water balance components using the WA + framework; (ii) characterise the spatial and temporal patterns of water availability, depletion, and consumption across the basin; (iii) examine *ET* partitioning and water use across land use classes and sub-basins; and (iv) derive key WA + indicators relevant to basin closure, water stress, and water management in the transboundary ZRB.

2. Description of study region

The ZRB spans approximately 1.4 million km^2 across eight countries in south-central Africa: Angola, Botswana, Malawi, Mozambique, Namibia, Tanzania, Zambia, and Zimbabwe. It is the largest river basin in the Southern African Development Community (SADC) and, as shown in Fig. 1, is generally divided into 13 sub-basins, including the Upper Zambezi, Barotse, Cuando, Kafue, Kariba, Luangwa, Shire, Tete, and Zambezi Delta, among others. The Zambezi River itself flows about 2574 km from its source in the Kaleni Hills of northwestern Zambia to its delta in Mozambique at the Indian Ocean (Beilfuss, 2012).

The climate of the basin is highly heterogeneous, reflecting a gradient from humid subtropical in the north-east to semi-arid in the south-west. Mean annual *P* ranges from over 1200 mm in the northern and eastern regions to less than 700 mm in the southwestern

Table 1
Data inputs for the water accounting plus (WA+) model for the ZRB.

No.	Data Type	Units	Dataset	Source	Temporal Resolution	Temporal Coverage
1	*P*	mm	CHIRPS v2.0 Final	Funk, et al., (2015)	Daily and monthly	2003—2023
2	ET_a	mm	SSEBop v6.1	Senay, et al., (2013)	Monthly	2003—2023
3	ET_p	mm	GLEAM v3.8a	Martens, et al., (2017); Miralles, et al., (2011)	Monthly	2003—2023
4	LULC	N/A	ESA CCI	ESA, (2017)	Annual	2003—2020
5	LAI	m^2/m^2	MOD15A2H.006	Myneni, et al., (2015)	Monthly	2003—2023
6	NPP	kg m^{-2} yr^{-1}	MOD17A3HGF v006	Running and Zhao, (2019)	Monthly	2003—2023
7	GPP	kg m^{-2} yr^{-1}	MOD17A2Hv006	Running et al., (2015)	Monthly	2003—2023
8	Saturated Water Content (ThetaSat)	m^3/m^3	HiHydroSoil v2.0	Simons et al., (2020)	Static	2020
9	DEM	m	HydroSHEDS v1 DEM	Lehner et al., (2008)	Static	Published in 2008 (derived from Shuttle Radar Topography Mission (SRTM) collected in 2000)
10	NDM	kg/ha	N/A	Calculated from GPP and NPP	Monthly	2003—2023
11	EWR	%	N/A	Smakhtin et al., (2004)	Static	1961–1990 long-term reference period
12	Irrigated areas	%	GMIA	FAO, (2024)	Static	2005
13	Grey water fraction	N/A	WPL	Liu, et al., (2012)	Static	2000
14	Protected area boundaries	N/A	World Database on Protected Areas (WDPA)	WDPA, (2023)	Static	2023
15	Managed water bodies	N/A	Global Reservoir and Dam Database (GRanD)	Lehner, et al., (2011)	Static	2011
16	Basin outline	N/A	HydroBasins HydroBASINS / HydroSHEDS	Lehner and Grill, (2013)	Static	Published in 2013 (derived from Shuttle Radar Topography Mission (SRTM) collected in 2000)
17	Discharge	m^3/ second	N/A	Zambezi Watercourse Commission (ZAMCOM)	Monthly	2003—2023

parts of the basin. Regions closer to the Equator and the Indian Ocean receive the most rainfall, due to the influence of tropical convection and moisture-bearing winds from the ocean. In contrast, the southwestern parts of the basin are much drier. This spatial variation in climate leads to uneven water availability: the wetter upper basin and eastern parts of the basin generate substantial runoff, whereas major floodplains and open-water systems, such as Lake Malawi and the Barotse Floodplains, experience substantial evaporation losses (Beilfuss, 2012). The flow regime of the river is strongly seasonal, with a rainy season typically from November to April and a pronounced dry season. Major reservoirs (notably Lake Kariba and Cahora Bassa) on the Zambezi and its tributaries regulate flows for hydropower and have significant surface areas contributing to evaporation. Groundwater is an important component in some parts of the basin, with notable aquifers that provide baseflow and drought supply. Overall, the diverse climate and geography of the ZRB result in complex hydrology that necessitates integrated analysis at the basin scale.

The ZRB waters are critical for poverty alleviation and sustainable economic growth within the region because they meet the needs of over 30 million people while sustaining a rich and diverse natural environment (Beilfuss, 2012). The population of the basin is unevenly distributed, with over 85% of people living in Malawi, Zambia and Zimbabwe, and within four sub-basins, namely the Kafue, Kariba, Tete and the Shire (World Bank, 2010). The main economic activities are agriculture, mining, fishing, tourism and manufacturing.

3. Materials and methods

In this study, the WA + framework, which is based on the mass water balance, was deployed for the ZRB boundary for the period 2003–2023. The data inputs were available at daily, monthly and annual time steps, whereas other inputs were static (Table 1). All spatial datasets were resampled to a resolution of approximately 1 km. The following section describes the main and intermediate datasets used, the WA + model and the indicators calculated.

3.1. Data inputs

The WA + framework utilises several freely available satellite datasets. The main temporal datasets include four hydroclimatic variables, LULC and three satellite vegetation indices. The hydroclimatic data inputs of the framework were precipitation (P), ET_a, potential evapotranspiration (ET_p) and basin discharge. The vegetation indices include leaf area index (LAI), net primary production (NPP), and gross primary production (GPP). The static datasets include saturated water content (ThetaSat), digital elevation model (DEM), environmental water requirement (EWR), global map of irrigated areas (GMIA), water pollutant load (WPL), protected area boundaries and the basin boundary. The model also computes intermediate datasets that are created in the earlier stages of deployment. These include the number of rainy days (nRD), net dry matter (NDM) and interception. Table 1 provides a summary of the main data inputs used in the ZRB water accounting process.

The WA + framework utilises daily and monthly P. This study utilised P from the Climate Hazard Infra-red Precipitation with Stations (CHIRPS) (Funk, et al., 2015) for the period 2003–2023. For the African Continent, CHIRPS is considered as a reliable source of satellite rainfall estimates (Bamweyana et al., 2021; Mekonnen, et al., Accuracy of satellite and reanalysis rainfall estimates over Africa: A multi-scale assessment of eight products for continental applications, 2023). P is a primary input of the WA + as it represents the main inflow of water in a basin. Monthly P was used to calculate the annual gross rainfall of the basin. The daily P was used to determine the monthly nRD, which is used to calculate interception in the WA + framework.

Remotely sensed ET_a is an essential input to the WA + framework because it is used to estimate and monitor trends in consumptive water use and water withdrawals in a basin where water accounting is executed (Karimi et al., 2019). ET_a produced using the SSEBop model was used in this study. SSEBop is based on and is a parameterisation of the Simplified Surface Energy Balance (SSEB) approach that utilises predetermined boundary conditions that are distinctive to each pixel for the warm and cold reference conditions (Senay, et al., 2013).

The ET_p data used in the study were the Global Land Evaporation Amsterdam Model (GLEAM) version 3.7 (Martens, et al., 2017; Miralles, et al., 2011). GLEAM is a set of algorithms that estimate terrestrial evaporation and root-zone soil moisture using remote sensing data (Martens, et al., 2017). GLEAM v3.7 is different from the first version because it includes a revised formulation of the evaporative stress, an optimised drainage algorithm and a new soil moisture data assimilation system (Martens, et al., 2017). The ET_p is used when identifying blue and green water pixels.

LULC is a crucial input and component of the WA + framework as it combines how land is being used with how water is used across the landscape. This is used to determine which portions of water are manageable and non-manageable (Dembélé, et al., 2023). In this study, the European Space Agency (ESA) Climate Change Initiative (CCI) land cover products (ESA, 2017) from 2003 to 2020 were reclassified to the WALU classes. The WA+ framework utilises three remote sensing vegetation indices. These include LAI, GPP and NPP. During the water accounting process, LAI was used in the estimation of interception. The LAI defined as the green leaf area per unit ground area (Myneni, et al., 2002) used in this study was obtained from the Moderate Resolution Imaging Spectroradiometer (MODIS) MOD15A2H Version 6 product (Myneni et al., 2015). GPP and NPP quantify the rate at which carbon dioxide is converted into plant biomass (Running, et al., 2004) through the process of photosynthesis within a given ecosystem over a specified period. GPP and NPP were used to determine NDM, which was combined with the interception to estimate transpiration during the process of partitioning ET into its individual components.

The WA+ framework uses several static datasets. Saturated water content was obtained from the HiHydroSoil (Simons et al., 2020) database. It was used during the process of soil moisture modelling. The DEM was obtained from hydroshed and was used to model runoff within the basin. EWR is the total volume of water required to sustain freshwater ecosystem functions and the services supplied

to humanity (Smakhtin et al., 2004). The dataset was obtained from IWMI and was used to estimate the reserved outflow, which is one of the indicators produced during the water accounting process. The GMIA dataset gives the areas under irrigation, expressed as a percentage (FAO, 2024). It was used to determine blue ET (ET_{blue}) *within* the model. Protected area boundaries were acquired from the World Database on Protected Areas (WDPA) (WDPA, 2023) and were used to determine conservation zones that experienced little land modification and water management.

3.2. Data preprocessing and WA+ implementation workflow

The WA+ implementation followed the Scale-Invariant Water Accounting Plus (SIWA+) approach (Owusu, et al., 2025; Mekonnen, et al., 2026; Patle et al., 2023; Karimi et al., 2019), adapted to the ZRB. All spatial datasets were harmonised to a common basin-wide analysis grid. Since the analysis was undertaken in EPSG:4326 (WGS 84 geographic coordinate system), the working grid used an angular cell size chosen to approximate 1 km at the basin scale. Continuous variables were resampled using bilinear interpolation, while categorical variables were resampled using nearest-neighbour interpolation to preserve class integrity. Monthly variables were aggregated to the annual time step required for the WA + sheets and trend analyses.

No additional bias correction was applied to CHIRPS or SSEBop within the WA + workflow. Likewise, no temporal gap-filling was applied to these gridded products. The only gap-filled dataset used in the broader study context was discharge, which is discussed separately under the Validation and uncertainty assessment subsection. P and ET_a were used to calculate the *surface water yield* (P - ET_a).

Monthly nRD was computed as the count of days within each month on which daily precipitation was greater than or equal to 0.254 mm (0.01 in.), a commonly used threshold for measurable precipitation, applied here to exclude trace rainfall amounts and reduce the influence of very small satellite-derived precipitation estimates. This rainy-day frequency, together with monthly precipitation and LAI, was then used to estimate monthly interception following the WA + methodology. Monthly transpiration and evaporation were subsequently derived within the same framework, using NDM and interception as intermediate inputs, and annual values were obtained by summing the monthly components.

3.3. WA + land use and land cover

Land use/land cover (LULC) are a key input for the WA + framework. Within the WA + framework, LULC is first converted into standard Water Accounting Land Use (WALU) classes via a lookup table that combines the water use with land use. The reclassified layer is subsequently intersected with the WDPA, GMIA and GRanD layers (Lehner et al., 2011; FAO, 2024; WDPA, 2023) to identify protected land-use classes, irrigated areas, and managed water bodies, respectively. WALU classes are grouped into four broad categories, namely protected land use (PLU), utilised land use (ULU), modified land use (MLU) and managed water use (MWU) (Karimi et al., 2013a). PLU refers to protected areas that are pristine and environmentally sensitive such as national parks and RAMSAR sites; ULU relates to areas with minimal human influence such as shrublands and wetlands; MLU refers to an area where the original land use has been replaced by humanity to improve its utility such as rainfed croplands; and MWU relates to areas where water has been diverted using man-made infrastructure such as dams and canals (Bastiaanssen et al., 2015). In this study, annual ESA CCI land cover (ESA, 2017) products from 2003 to 2020 were reclassified into the WALU classes (Table 2 and Fig. 2).

It should be noted that at the time of the original analysis, annual ESA CCI LULC maps were only available for the period 2003–2020, whereas the hydroclimatic inputs used in the WA + analysis were available through 2003–2023. To maintain temporal consistency in the WALU-dependent components of the framework, the 2020 LULC map was carried forward for 2021–2023.

Table 2
WALU classes within the ZRB.

WA + LULC	Area (km^2)	Area (%)	WALU	Area (km^2	Area (%)
Protected forests	213,442.14	17%	Protected Land Use (PLU)	422,716.82	33%
Protected shrublands	137,434.92	11%			
Protected wetlands	110.19	0%			
Protected other	71,729.56	6%			
Closed deciduous forest	220,268.54	17%	Utilised Land Use (ULU)	742,679.48	58%
Open deciduous forest	172,686.48	13%			
Closed evergreen forest	469.42	0%			
Open evergreen forest	315.15	0%			
Shrub land & mesquite	214,437.18	17%			
Herbaceous cover	92,378.46	7%			
Meadow & open grassland	41,634.99	3%			
Bare soil	460.60	0%			
Wetlands	28.65	0%			
Rainfed crops - cereals	63,587.47	5%	Modified Land Use (MLU)	77,267.82	6%
Mixed species agro-forestry	13,680.35	1%			
Irrigated crops - cereals	12,452.81	1%	Managed Water Use (MWU)	46,115.40	4%
Managed water bodies	31,566.74	2%			
Urban paved Surface (lots, roads, lanes)	2095.85	0%			

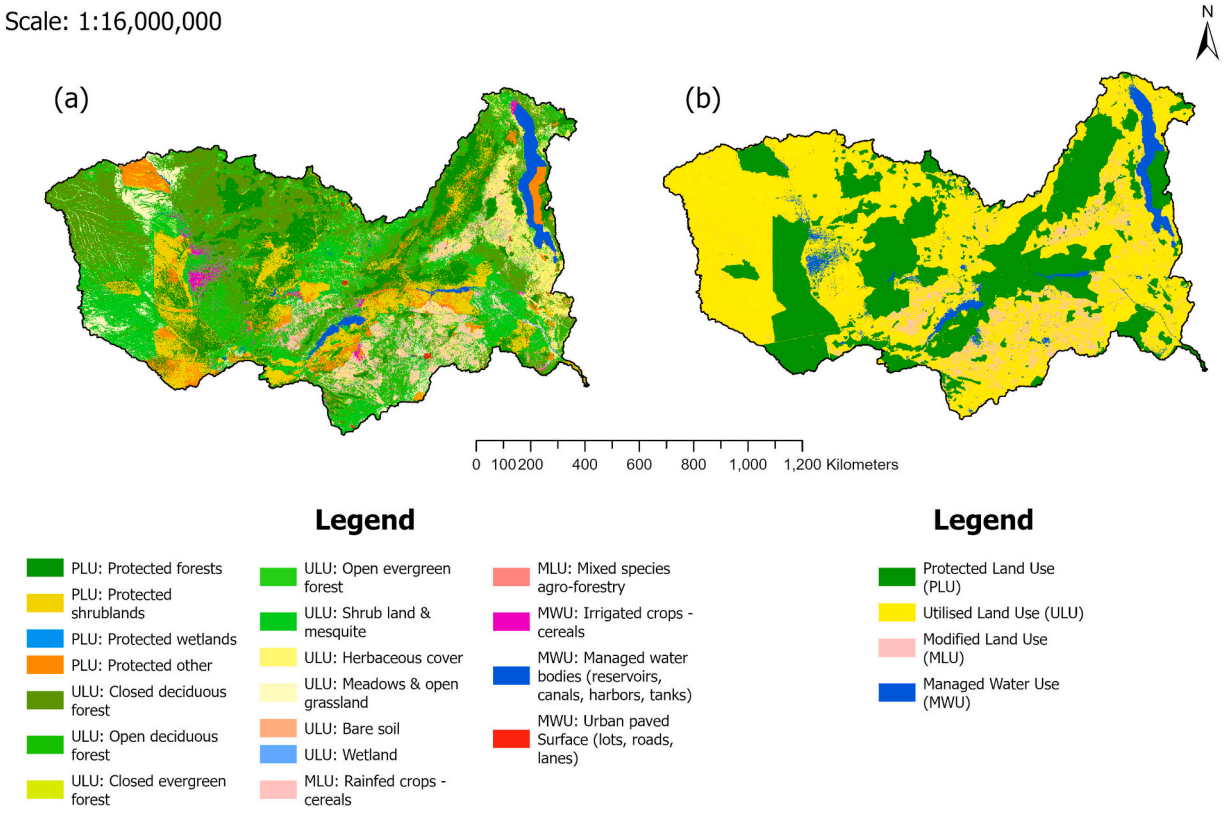


Fig. 2. Water accounting land use classes across the ZRB.

3.4. Determination of green and blue ET within the WA + Framework

In the WA + , blue and green ET (ET_{blue} and ET_{green}) are differentiated by water source. ET_{blue} (incremental ET) originates from blue water resources, such as aquifers, lakes, reservoirs, and irrigation supplies, whereas ET_{green} (rainfall ET) originates from the green water resource, which is the moisture in the soil. As implied, vegetation ET originates from rainfall stored as soil moisture and used by vegetation or evaporated from the soil surface (Falkenmark and Rockström, 2006; Velpuri and Senay, 2017). Total actual evapotranspiration (ET_a) was therefore partitioned as the sum of ET_{blue} and ET_{green}:

$$ET_a = \quad ET_{blue} + ET_{green} \tag{1}$$

In WA + , ET_a is partitioned into ET_{green} and ET_{blue} using a water-balance approach. Under this approach, ET_{blue} is estimated as the residual of rainfall-based soil-moisture balance when ET_a exceeds the water available from rainfall, while ET_{green} is the remaining rainfall-supported component of ET_a. This is consistent with recent WA + applications by Owusu et al. (2025) and Mekonnen et al. (2026), which describe ET_{blue} as the negative soil-moisture residual and ET_{green} as the remainder of ET_a after ET_{blue} is removed.

Monthly ET_{blue}, ET_{green}, and soil moisture were calculated using Eqs. (2) – (4):

$$ET_{blue} = \begin{cases} 0, \&if(SM_t \geq 0) \\ (SM_t \times -1), \&if(SM_t < 0) \end{cases} \tag{2}$$

$$ET_{green} = \begin{cases} ET_a, \&if(SM_t > ET_a) \\ ET_a - ET_{blue}, \&if(SM_t < ET_a) \end{cases} \tag{3}$$

$$SM_t = SM_{t-1} + (P - I)_t - (ET_a - I)_t - QP_t - QS_r \tag{4}$$

where SM_{t-1} is soil moisture from the previous month, $(P - I)$ is effective precipitation after interception loss, I is interception, and QP and QS are rainfall-based percolation and surface runoff terms, respectively. Under this formulation, a negative soil-moisture balance indicates that ET_a exceeds rainfall-supported supply and that an additional blue-water source contributes to evapotranspiration. This partitioning is useful for assessing irrigation dependence and the relative contribution of green and blue water to consumptive use across WALU classes.

3.5. WA + sheets and indicators

The WA + framework produces outputs in the form of thematic sheets, tables and spatial layers. Two key thematic sheets that this study focused on are the resource base and evapotranspiration sheets.

3.5.1. Resource base sheet

The resource base sheet is a critical output of the WA + framework because it provides a summary of the water resources status of a given domain. The sheet can be used to provide baseline assessments of water resources, such as the establishment of a water budget for a given basin. The fundamental inflows accounted for include *P* and external subsurface and surface inflows- inter-basin transfers and desalinated water. These inflows comprise the total water that flows into a specified basin and are referred to as the *gross inflow*. However, the *gross inflow* does not account for surface and groundwater storage changes (*Δs*) in a given basin. The summation of the storage changes and the *gross inflow* is referred to as the *net inflow*. The *net inflow* is either depleted by the landscape or can be exploited. Hence, it is divided into *landscape ET* and *exploitable water*. *Landscape ET* is a result of different rainfall distributions across diverse geologies, land uses, soil formations, topologies, topographies and drainage systems (Karimi et al., 2013a). *Landscape ET* is depleted and is unusable downstream. *Landscape ET* is composed of the green and blue *ET*, which are depleted across the different WALU classes.

Exploitable water is the part of the *net inflow* that is not evaporated and is available for use downstream within the soil, streams and aquifers (Karimi et al., 2013a). However, a share of the *exploitable water* is reserved to meet the maximum downstream water obligations and therefore considered unavailable. These obligations may include environmental flows and inter-basin transfers out of the basin. The reserved portion of the *exploitable water* is referred to as the *reserved outflow (*Karimi et al., 2013a*)*. *Non-utilisable outflow* is also unavailable for use downstream, and is considered as excess water that usually emerges during and after floods and has to be expelled from the basin as quickly as possible. After accounting for the *reserved* and non-*utilisable outflow,* the left over is known as *available water (*Bastiaanssen et al., 2015*),* which can be used within a basin. *Available water* is comprised of what is actually used by different water users and sectors (*utilised flow*) and surplus water that is not consumed and still available for future consumption. (Karimi et al., 2013a; Bastiaanssen et al., 2015). The key outflows depicted on the resource base sheet are depleted water as *ET*, river outflow, and exported water in the form of inter-basin transfer out of the basin.

3.5.2. ET Thematic sheet

ET is the largest outflow in many basins, and it is crucial in comprehending water use efficiency and productivity (Karimi et al., 2013a). The ET sheet provides a comprehensive description of water consumption through *ET* because it accounts for the *ET* processes that are managed, manageable or non-manageable. The ET sheet also provides the portions of water consumed in sectors such as agriculture. Because *ET* is partitioned into evaporation, interception and transpiration in the WA + framework, it is possible to distinguish between *beneficial* and *non-beneficial ET* (Dembélé, et al., 2023). *Beneficial ET* is the portion of ET that supports productive consumption, such as water consumed by crops (*agriculture ET*) and natural vegetation such as forests (*environmental ET*). *Non-beneficial ET* does not support productive consumption and refers to processes such as open-water and bare-soil evaporation. Interception is assumed to be mostly non-beneficial, even though it can be beneficial in processes such as temperature regulation of plants (Karimi et al., 2013a). Transpiration is mainly beneficial because it indicates the water that is consumed by plants for photosynthesis and biomass production. This is primarily for beneficial biomass production in crop fields, rangelands, and forests.

3.6. WA+ performance indicators

The WA+ performance indicators used in this study were selected to characterise basin conditions across three complementary dimensions: ecological pressure, agricultural water use and productivity, and physical water availability. Together, these indicators provide a concise, policy-relevant summary of basin status while remaining clear and interpretable for water management purposes. Recent WA+ applications have similarly used compact indicator sets to summarise water availability, ecological requirements and beneficial water use (Owusu, et al., 2025; Mekonnen, et al., 2026).

The Environmental Water Stress (EWS) was used as the principal ecological indicator. In the WA + framework, EWS represents the pressure on water resources after accounting for environmental flow needs, derived as the ratio of utilised flow to the difference between exploitable water and environmentally reserved outflows. For interpretive purposes, EWS classes were aligned with the environmental-flow-adjusted water-stress thresholds used in SDG Indicator 6.4.2, where water stress is interpreted as no stress (<25%), low (25–50%), medium (50–75%), high (75–100%), and critical (>100%) (FAO, 2024). Although the WA + EWS formulation is not identical to the SDG 6.4.2 indicator, both metrics express pressure on freshwater resources after accounting for environmental flow requirements, making these thresholds useful for interpretation (FAO, 2024; Mekonnen, et al., 2026).

In this study, three indicators were used to characterise agricultural water conditions. The *Evaporative Stress Index* (ESI) was used as a proxy for vegetation water stress, with higher values indicating stronger evaporative stress (Anderson, et al., 2016). The *Agricultural Evapotranspiration Fraction* (AEF) was used to show the proportion of total evapotranspiration attributable to agriculture (Dembélé, et al., 2023) and, therefore, the relative importance of agricultural water consumption within the basin water balance. The *Beneficial Fraction* (BF) was used to indicate the fraction of consumed water that directly contributes to productive transpiration and biomass generation (Karimi et al., 2013a; Dembélé, et al., 2023). Together, these indicators provide complementary information on agricultural water stress, the importance of agriculture in basin-scale water consumption, and the productive use of depleted water.

Two indicators were used to represent physical water scarcity and basin closure. *Water Availability Per Capita* (WAPC) was used as the per-capita indicator and was defined as available water divided by population, thereby expressing the volume of freshwater

available per person after accounting for reserved and non-utilisable outflows (Mekonnen, et al., 2026). *Basin Closure Fraction* (BCF) was used to indicate the proportion of exploitable water that is utilised within the basin. Higher BCF values indicate a greater degree of basin closure, while a value approaching 100% implies that nearly all available water resources are already utilised or stored, with little or no remaining outflow. Together, WAPC and BCF provide complementary information on human water availability and the overall pressure placed on basin water resources (Mekonnen, et al., 2026; Karimi et al., 2013a).

A summary of the retained indicators, including their interpretation and formulas, is provided in Table 3. Basin-scale trends in the annual indicators were evaluated using the Mann–Kendall test with Sen's slope, while linear trend magnitudes were additionally summarised using ordinary least squares (OLS) regression with associated p-values and 95% confidence intervals.

3.7. Validation and uncertainty assessment

Several supplementary checks were conducted to assess the robustness of the datasets and assumptions used in the WA + analysis, with an emphasis on the key inputs that influence basin-scale water accounting results, namely P, ET_a, LULC, and discharge.

The P forcing was assessed using an independent basin-wide evaluation of rainfall products for the ZRB. CHIRPS, MSWEP, ERA, RFE and TAMSAT were compared against station rainfall observations available within the basin over the validation period. Product performance was evaluated using complementary goodness-of-fit and error metrics, including Pearson's correlation coefficient (r), Kendall's Tau, root mean square error (RMSE), mean absolute relative error (MARE), percent bias (P-bias), Nash–Sutcliffe efficiency (NSE), Kling–Gupta efficiency (KGE), modified KGE and non-parametric KGE. These metrics were selected to assess linear association, rank association, error magnitude, relative error, bias and hydrological consistency. The comparison was used to evaluate the suitability of the P product used as WA + forcing and to characterise P-related uncertainty in the basin-scale water-balance results.

For the LULC component, annual ESA CCI maps were only available up to 2020 at the time of the original analysis, whereas the WA + assessment covered 2003–2023. To maintain temporal consistency in the WALU-dependent components of the framework, the 2020 LULC map was therefore carried forward for 2021–2023 under the assumption that basin-scale land-cover/use conditions did not change substantially during this period. The reasonableness of this assumption was evaluated through supplementary land-cover stability checks. The most recent observed ESA CCI-derived LUWA maps were compared within the ZRB boundary to assess class stability prior to the carry-forward period, while two independent Sentinel−2-based land-cover products, ESRI/Impact Observatory (ESRI and Impact Observatory, 2026) and Dynamic World V1 (Brown, et al., 2022), were used to compare land-cover stability and class-composition changes over two equivalent three-year windows, 2017–2020 and 2020–2023. The analysis was conducted at the basin scale and within the portions of riparian countries that fall within the ZRB, with FAOSTAT (FAO, 2026)land-cover statistics used as contextual national-level evidence. The carry-forward assumption is acknowledged as a source of uncertainty for class-based allocation and ET partitioning outputs in the final three years of the analysis, particularly for localised changes that may not be fully represented at the basin scale.

Discharge was assessed as an outlet-level uncertainty check for the runoff and surface-water outflow components of the WA + results. An independently reconstructed GRDC-based discharge series for the Zambezi outlet was used for this purpose. The reconstruction was developed in a separate discharge gap-filling study using historical daily observations for 1960–1990, with 5218 observations split into calibration and validation subsets (Tinonetsana et al. (n.d), unpublished results). In the present study, the reconstructed discharge series was not used to calibrate, adjust, or predict the 2003–2023 WA + water-balance outputs. Instead, only the independent validation-period performance at the Zambezi outlet was used to characterise uncertainty in discharge-based interpretation. Validation performance was evaluated using KGE, NSE, R^2, PBIAS and RSR. KGE, NSE, R^2 and RSR were used to assess the ability of the reconstructed outlet series to reproduce observed discharge dynamics, while PBIAS was used to assess mean-flow bias. The WA + surface-water outflow estimates for 2003–2023 were also compared with published long-term Zambezi runoff and discharge estimates to assess whether their magnitudes were hydrologically plausible. This assessment was therefore interpreted as an outlet-level constraint on surface-water uncertainty, rather than a direct validation of each annual WA + water-balance component.

Table 3
Summary of WA + performance indicators used in this study.

Indicator	Description	Formula
Environmental Water Stress (EWS)	Indicator of pressure on freshwater resources after accounting for environmental flow requirements. Higher values indicate greater ecological pressure.	$\frac{Utilised\ Flow}{Exploitable\ Water - Reserved\ Outflow}$
Evaporative Stress Index (ESI)	Proxy for vegetation water stress based on the degree to which actual evapotranspiration falls below potential evapotranspiration. Higher values indicate stronger evaporative stress.	$1 - \frac{ET}{PET}$
Agricultural ET fraction (AEF)	Share of total evapotranspiration attributable to agriculture, indicating the relative importance of agricultural water consumption within the basin water balance.	$\frac{Agricultural\ ET}{ET}$
Beneficial Fraction (BF)	The fraction of consumed water that contributes directly to productive transpiration and biomass generation. Higher values indicate a greater proportion of beneficial water consumption.	$\frac{T}{ET}$
Water Availability Per Capita (WAPC)	Volume of available water per person after accounting for reserved and non-utilisable outflows. Higher values indicate greater freshwater availability relative to population.	$\frac{Available\ Water}{Population}$
Basin Closure Fraction (BCF)	Proportion of exploitable water already allocated within the basin. Higher values indicate a greater degree of basin closure.	$\frac{Utilised\ Flow + Reserved\ Outflow}{Exploitable\ Water}$

Together, these indicators summarise key dimensions of basin water stress and use.

In addition, uncertainty was considered qualitatively for other key components of the analysis. The LULC carry-forward assumption for 2021–2023 was evaluated separately using a temporal harmonisation check (Supplementary Table S1).

4. Results

The results of the WA + analysis for the ZRB are presented as long-term averages and inter-annually. The resource base sheet summarised the annual variability of water stocks and flows, while the ET sheet summarised the variability in water consumption over the period. Sub-catchment-level distributions and contributions are summarised, and their WA + indicators are computed.

4.1. Validation and uncertainty assessment

The basin-wide rainfall product evaluation indicated that the CHIRPS dataset used in the WA + analysis performed well over the ZRB (Supplementary Table S1). CHIRPS achieved Pearson's r = 0.8897, Tau = 0.8079, RMSE = 50.0827 mm, MARE = 0.3226, P-bias = −0.6119%, NSE = 0.7905 and KGE = 0.8646, indicating strong agreement with station observations, low bias and good hydrological performance. MSWEP showed similarly strong performance, with slightly higher Pearson's r (0.8904), lower RMSE (49.9717 mm) and higher NSE (0.7925), although its KGE (0.8326), Tau (0.7668) and P-bias (−1.5421%) were weaker than CHIRPS. RFE and TAMSAT showed moderate but lower overall performance, with KGE values of 0.7957 and 0.7975 and NSE values of 0.7418 and 0.7192, respectively. ERA performed weakest overall, particularly in terms of bias and efficiency, with P-bias = 13.7752%, NSE = 0.6894 and KGE = 0.6727. Although MSWEP performed comparably to CHIRPS in several metrics, CHIRPS was retained because it combined high correlation, the lowest absolute bias, strong NSE and the highest KGE among the tested products, while also providing a finer native spatial resolution (0.05°) than MSWEP (0.1°) and maintaining consistency with the WA + processing chain. This finding is consistent with broader rainfall-product validation work over Africa, which shows that product performance varies by region, timescale and metric, and that CHIRPS, MSWEP and RFE are among the more reliable products for rainfall climatology and hydrological applications, whereas ERA-type reanalysis products may show weaker performance in capturing in situ rainfall variability in some settings (Mekonnen, et al., 2023).

The SSEBop v6.1 estimates produced a mean annual basin-wide ET_a of 1095.6 $km^3\ yr^{-1}$ over 2003–2023, with annual values ranging from 976.7 $km^3\ yr^{-1}$ in 2005–1324.5 $km^3\ yr^{-1}$ in 2022. These magnitudes are hydrologically plausible for the ZRB because recent Africa-focused ET studies emphasise that ET_a is a central component of the terrestrial water balance and the dominant consumptive flux in many African catchments, often accounting for most annual precipitation (Zimba, et al., 2023; Akpoti, et al., 2026). The use of SSEBop v6.1 is further supported by its operational basis as a simplified surface energy balance model that combines thermal remote sensing with weather data to estimate actual ET at large spatial scales (Senay, et al., 2013). Africa-wide product evaluations also support the use of SSEBop for basin-scale applications. Weerasinghe et al. (2020) ranked SSEBop among the highest-performing ET products over Africa because of its low bias and good representation of spatial variability, while Akpoti et al. (2026) benchmarked SSEBop v6.1 against MODIS16, WaPOR and GLEAM across African climate zones, land-use classes and major river basins, including the Zambezi, and found that SSEBop generally aligned well with other major ET_a products. At the local scale, Zimba et al. (2023) showed that satellite-based ET products, including SSEBop, can reproduce aspects of seasonal evaporation behaviour in miombo woodland, although with phenophase-dependent uncertainty. These studies support the suitability of SSEBop v6.1 for basin-scale WA + assessment in the ZRB, while also confirming that ET_a remains an important source of uncertainty, particularly over heterogeneous woodland, wetland, irrigated and seasonally water-stressed landscapes.

The supplementary LULC stability assessment indicated that the 2020 carry-forward period did not show greater basin-scale instability than the preceding observed period (Supplementary Table S2a). The ESA CCI-derived LUWA comparison showed very high stability between 2017 and 2020, with 99.52% of valid basin pixels retaining the same detailed LUWA class and only 0.48% changing class. The independent Sentinel−2-based products showed lower pixel-level stability, as expected for higher-resolution products, but their behaviour was consistent across the two three-year windows. For ESRI/Impact Observatory, stable pixels increased from 86.47% in 2017–2020–87.06% in 2020–2023, while changed pixels decreased from 13.53% to 12.94%. Dynamic World showed a similar pattern, with stable pixels increasing from 84.83% to 85.58% and changed pixels decreasing from 15.17% to 14.42%. These results suggest that the 2020–2023 period was not characterised by greater basin-scale LULC instability than the 2017–2020 period, supporting the use of the 2020 ESA CCI-derived LUWA layer as a carry-forward representation for the final three years of the WA + analysis, while recognising that localised changes may remain unresolved.

The FAOSTAT comparison provided broadly consistent contextual evidence, particularly in showing limited change across the cropland, water, wetland/flooded vegetation, built-up, and bare/sparse classes (Supplementary Table S2b). For the riparian countries combined, the FAOSTAT MODIS-based series showed relatively small class-composition changes during 2017–2020, with the largest shifts occurring in trees/forest (−0.47 %age points), grass/shrub/rangeland (+0.36 %age points) and bare/sparse land (+0.24 %age points). During 2020–2023, FAOSTAT again indicated that the main change was between trees/forest and grass/shrub/rangeland, which changed by −1.31 and + 1.27 %age points, respectively, while cropland changed by only + 0.05 %age points and water, wetland/flooded vegetation, built-up and bare/sparse classes each changed by less than 0.05 %age points. This pattern is consistent with the remote-sensing results, indicating that the most apparent change was concentrated in vegetation-related classes rather than in major shifts in agricultural, built-up, or water-related land-cover classes.

The outlet discharge assessment provided useful, though cautious, evidence for interpreting uncertainty in the WA + surface-water outflow estimates. For the independent validation period, the reconstructed Zambezi outlet discharge yielded KGE = 0.52, NSE = 0.03, R^2 = 0.03, PBIAS = −4.2% and RSR = 0.98 (Supplementary Table S3). The KGE indicates satisfactory overall performance,

and the low PBIAS indicates limited mean-flow bias; however, the low NSE and R^2, together with the high RSR, indicate reduced ability to reproduce detailed daily flow variability. This suggests that the reconstructed discharge series is more useful as an outlet-level constraint on mean-flow plausibility than as a precise benchmark for high-frequency discharge dynamics. The WA + surface-water outflow estimates for 2003–2023 averaged 69.0 $km^3\ yr^{-1}$, ranging from 30.0 $km^3\ yr^{-1}$ in 2023–86.6 $km^3\ yr^{-1}$ in 2013. These values are lower than published estimates of natural long-term Zambezi runoff but remain within the same broad order of magnitude as reported Zambezi flow volumes. FAO (1997) approximately 77.5 $km^3\ yr^{-1}$ entering Lake Cahora Bassa from the upstream Zambezi system, with a further contribution of nearly 16 $km^3\ yr^{-1}$ from the Shire system, while Beilfuss (2012) reports total natural annual runoff for the ZRB of approximately 110.7 $km^3\ yr^{-1}$. Overall, the discharge assessment supports the broad plausibility of the WA + surface-water outflow estimates and confirms that runoff and outflow components should be interpreted with caution, particularly regarding annual variability.

4.2. Water account of the Zambezi River Basin

4.2.1. Average resource base thematic sheet and water balance components (2003–2023)

The WA + analysis of the ZRB underscores the predominant role of *P* in the basin water balance. The long-term average (2003–2023) resource base sheet, as shown in Fig. 3, reveals that *P* constitutes the largest water inflow, providing an annual average value of 1280.5 km^3. When this volume is distributed across an area of ~1.37 million km^2, it corresponds to an annual precipitation of ~932.5 mm, indicating a relatively moist basin. *P* serves as the primary source of water in the ZRB and represents the *gross inflow*. A substantial volume of water is lost to change in storage (*ΔS)*, averaging 115.9 km^3 annually, which reflects positive net storage change within the basin. This loss to *ΔS* results in a *net inflow* of 1164.6 km^3.

On average, *landscape ET* accounts for 91% of the *net inflow*, encompassing 1058.0 km^3 of water annually. On the other hand, *exploitable water* represents 106.6 km^3 of *net inflow*. ET_{green} accounts for 70% (763 km^3) of *landscape ET*, whereas ET_{blue} accounts for 30% (332.5 km^3), indicating greater dependence on *P* than on blue water sources within the basin. Both green and blue *ET* are mainly depleted in ULU, at 428 km^3 and 185 km^3, respectively.

Of the maximum *exploitable water*, the *available water* accounts for 86.4 km^3, representing 81%, leaving only 19% of *exploitable water* as reserved to meet water obligations, such as environmental flows, or is non-utilisable and evacuated from the basin. The *utilised flow* amounts to 44.5 km^3 and indicates blue water utilisation in the basin.

The total long-term average outflow of the ZRB is 1164.6 km^3 annually, and the main mode of water outflow is through *surface water outflow* via the Zambezi River into the Indian Ocean. The *surface water outflow* is 69.0 km^3 annually, and translates to 6% of the outflow. ET_a is the largest component of outflow, accounting for 1095.6 km^3 (94%) of the total outflow of the ZRB.

4.2.2. Spatial distribution of water balance components

The average spatial distribution of *P* and ET_a across the ZRB is shown in Fig. 4. *P* exhibits an uneven distribution, with higher concentrations in the northern and far eastern regions, due to their proximity to the equator and the influence of warm, moisture-laden winds from the Indian Ocean. ET_a exhibits a similar distribution, but is also elevated over open water bodies and wetlands, such as Lake

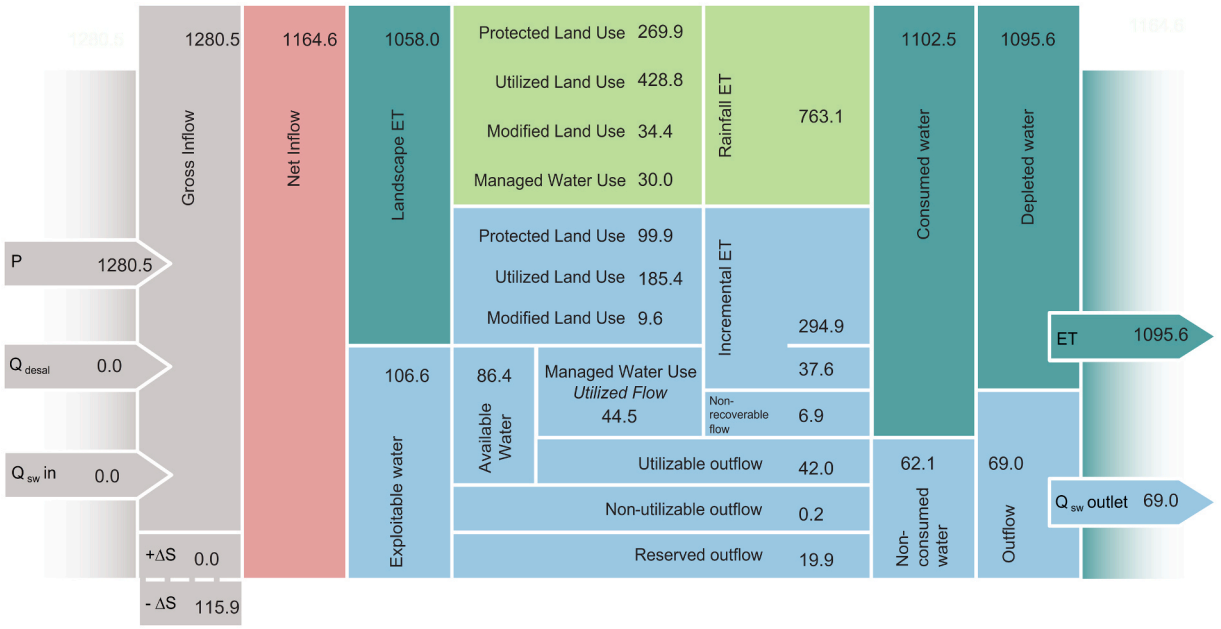


Fig. 3. Average resource base sheet of the ZRB for the period 2003–2023.

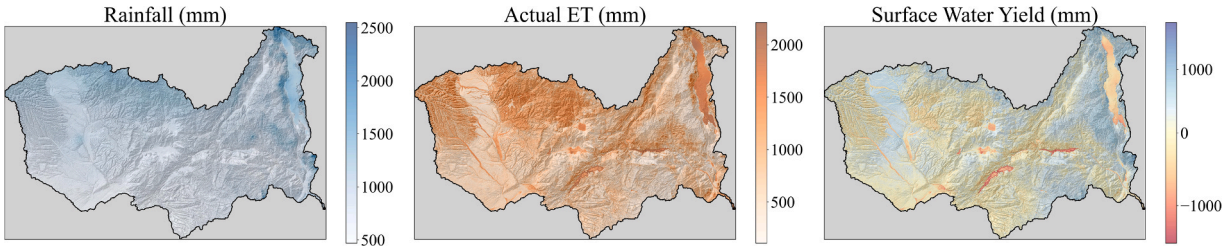


Fig. 4. Average spatial distributions of *P, ET_a* and *surface water yield*.

Malawi and the floodplains in the western part of the basin. Consequently, the *surface water yield* exhibits a gradient that increases from east to west, with negative values observed over open water surfaces and large wetland areas.

The averages of *P, ET_a* and *surface water yield* were also determined for the various WALU classes, primarily in areas that have remained stable without significant LULC changes from 2003 to 2023, to isolate hydroclimatic differences among classes and avoid conflating them with changes driven by land-cover transitions. The annual average *P* for the PLU, ULU, MLU, and MWU classes were found to be 899.6 mm, 951.9 mm, 810.1 mm, and 1083.4 mm, respectively. *P* is highest in the MWU class, which includes irrigated cereals, managed water bodies, and urban paved surfaces. Conversely, *P* is lowest in the MLU class, as most of this land use occurs in the southern part of the basin, where rainfall is less concentrated. The annual average ET_a for the PLU, ULU, MLU, and MWU classes were 819.8 mm, 775.3 mm, 535.4 mm, and 1400.7 mm, respectively. The higher ET_a in the MWU class can be attributed to the extensive open water surfaces and higher rainfall concentrations. Conversely, the lower ET_a in the MLU class is linked to its location in areas with lower rainfall. Consequently, *surface water yield* was lowest in the MWU class, as ET_a exceeded *P*. *Surface water yield* was −317.3 mm in MWU, 79.8 mm in PLU, 176.6 mm in ULU, and 274.7 mm in MLU. Despite the lower rainfall in MLU, *surface water yield* was highest due to the significantly lower ET_a. This reflects the fact that MWU areas are sustained not only by local rainfall but also by additional blue-water inputs, including stored or diverted surface water. As a result, MWU landscapes act as net zones of water consumption rather than net generators of surface water yield.

The average spatial distribution of ET_{blue} and ET_{green} across the ZRB is illustrated in Fig. 5. Spatially, ET_{blue} is predominantly concentrated over open water surfaces, while ET_{green} is primarily located in the northern regions of the basin, owing to their high vegetation cover. ET_{blue} is also elevated in the densely vegetated areas in the northwest of the basin, whereas ET_{green} is minimal over open water surfaces. This highlights the importance of open-water evaporation as a major component of non-rainfall-driven water loss in the basin. By contrast, ET_{green} was more extensive in vegetated parts of the basin, where evapotranspiration is primarily supported by rainfall and soil moisture.

Regarding land use, ET_{blue} is highest in the MWU class, which includes open water surfaces, at an annual average of 780.6 mm. In contrast, ET_{blue} is 232.9 mm, 222.2 mm, and 125.5 mm in the ULU, PLU, and MLU classes, respectively. The low ET_{blue} in MLU is primarily due to the predominance of rainfed cereals and mixed-species agroforestry, which are not irrigated. Despite MLU being largely composed of rainfed cereals and mixed-species agroforestry, ET_{green} remains relatively low at 409.9 mm annually, due to the low concentration of rainfall in this WALU class. ET_{green} is highest in the MWU class at 620.1 mm annually, owing to the high rainfall concentration in this class, and despite the presence of extensive open water surfaces. ET_{green} is also 597.6 mm in PLU and 542.4 mm in ULU.

4.2.3. Trends in water balance components

At the basin scale, inter-annual analysis indicates a general downward tendency in *P* (Fig. 6) and an upward tendency in ET_a over 2003–2023, although these basin-wide trends were not statistically significant according to the Mann–Kendall test or the OLS slope

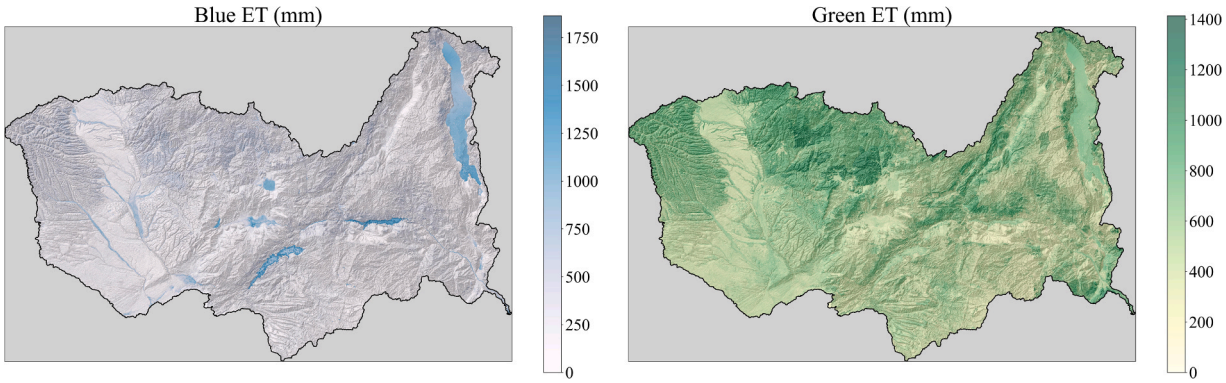


Fig. 5. Average annual spatial distribution of ET_{blue} and ET_{green}.

confidence intervals (Table 4). Specifically, *P* showed a Mann–Kendall p-value of 0.29 and an OLS slope of −2.63 km³ per year (95% confidence interval (CI): −12.17–6.91), while ET_a showed a Mann–Kendall p-value of 0.74 and an OLS slope of 3.49 km³ per year (95% CI: −2.68–9.65). Notably low rainfall was recorded in 2005, 2015, and 2023, with annual values of 1053.9 km³ , 1075.6 km³ , and 1170.9 km³ , respectively. In contrast, ET_a reached particularly high levels in 2022 and 2023, at 1324.5 km³ and 1216.7 km³ , respectively. Consequently, 2023 recorded the lowest *surface water yield* at −45.6 km³ , representing the only instance of negative *surface water yield* at the basin level during the study period. *ET* components also showed contrasting tendencies, with ET_{green} generally following rainfall variability, while ET_{blue} increased during high-ET_a years, particularly in 2022 and 2023. The lowest ET_{green} was recorded in 2005 (690.0 km³), coinciding with the year of lowest precipitation, whereas ET_{blue} peaked in 2022 and 2023 at 506.0 km³ and 494.6 km³ , respectively. By contrast, *exploitable water* and *available water* showed statistically significant negative OLS trends, with slopes of −1.42 km³ per year (95% CI: −2.57 to −0.28) and −1.40 km³ per year (95% CI: −2.52 to −0.27). In 2023, *exploitable water* and *available water* reached their lowest levels, recorded at 61.2 km³ and 43.2 km³ , respectively. In that year, *available water* constituted only 71% of *exploitable water*, substantially lower than the 81% average over the entire study period.

4.2.4. The evapotranspiration thematic sheet

The WA + ET sheet for the ZRB provides a detailed breakdown of the mean annual ET_a of 1095.6 km³ per year reported in the resource base sheet. This breakdown translates total water consumption into three WA + categories: *non-manageable*, *manageable*, and *managed ET*. Over the period 2003–2023, *manageable ET* accounted for the largest share of ET_a, averaging 614.1 km³ per year, or 56.0% of total ET_a. *Non-manageable ET* averaged 369.9 km³ per year, equivalent to 33.8% of total ET_a, while *managed ET* averaged 111.6 km³ per year, representing 10.2% of total ET_a (Fig. 7). This distribution shows that more than half of the water consumption in the basin occurred in land-use classes where management interventions can potentially influence water depletion, while approximately one-third occurred in non-manageable land uses, largely associated with protected and natural systems.

Transpiration varied across the three ET categories, indicating differences in the degree to which water consumption contributed directly to biomass production. In the non-manageable ET category, transpiration averaged 141.5 km³ per year, representing approximately 38.3% of *non-manageable ET*. A similar proportion was observed in the *manageable ET* category, where *transpiration* averaged 231.4 km³ per year and accounted for about 37.6% of *manageable ET*. In contrast, *transpiration* within the *managed ET* category averaged only 23.4 km³ per year, equivalent to 20.9% of managed ET. The lower share of *transpiration* in *managed ET* reflects the presence of non-transpirative or weakly transpirative surfaces, including managed water bodies, impervious urban areas, and other MLU and MWU classes. Overall, *transpiration* accounted for approximately 36.2% of total ET_a, highlighting its importance as the productive component of basin-wide water consumption.

The distinction between *beneficial* and *non-beneficial ET* further illustrates the productivity of consumed water in the basin. Over the study period, 554.3 km³ per year of *ET*a was classified as beneficial, while 541.3 km³ per year was classified as *non-beneficial*. This near-even split indicates that approximately half of the total ET_a contributed directly to biomass production, while the remainder was depleted through evaporation, interception, or other non-transpirative processes. *Beneficial ET* was dominated by *transpiration*, which accounted for approximately 71.5% of the *beneficial ET* category. The relatively high non-beneficial component indicates scope for improving the productive use of depleted water, particularly in managed and agricultural landscapes, while recognising that a portion of *non-beneficial ET* is unavoidable and hydrologically important in wetlands, forests, open-water systems, and other natural

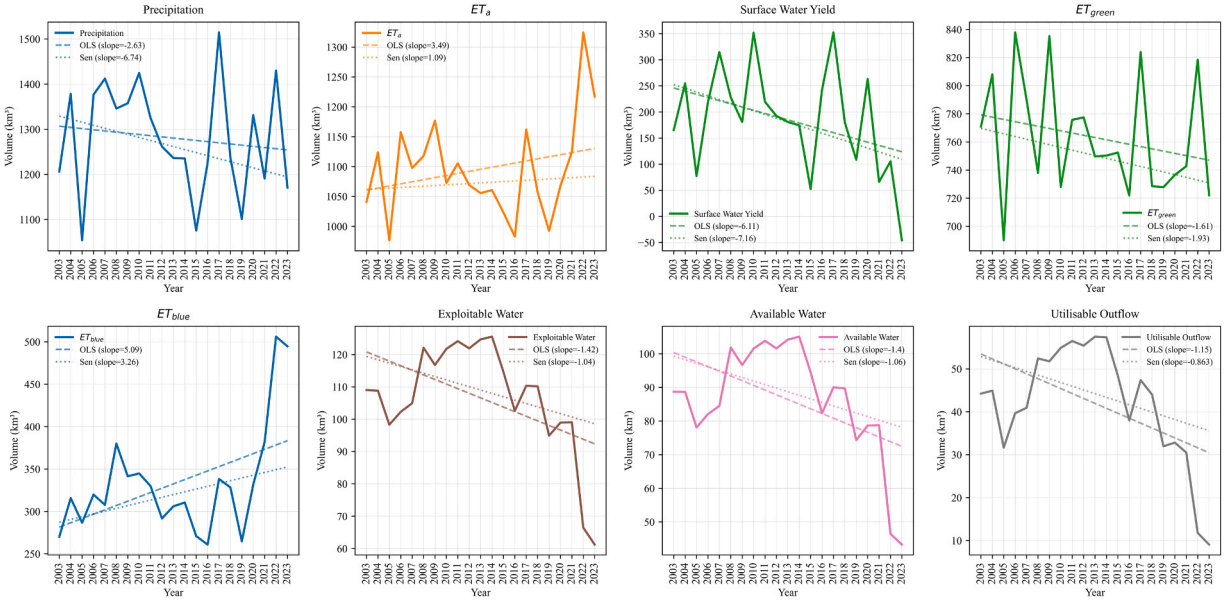


Fig. 6. Inter-annual basin-scale variation and fitted trend lines for selected water-balance components in the ZRB (2003–2023).

Table 4
Basin-scale trend statistics and key annual values for selected WA + indicators, 2003–2023.

Indicator	Unit	Mann–Kendall p-value	Mann–Kendall result	OLS slope	95% CI of OLS slope	Sen's slope	Interpretation
Precipitation (*P*)	km³ yr⁻¹	0.29	No significant trend	−2.63	−12.17–6.91	−6.74	Downward tendency, but not statistically significant
Actual ET (ET_a)	km³ yr⁻¹	0.740	No significant trend	3.49	−2.68–9.65	1.09	Upward tendency, but not statistically significant
Surface water yield	km³ yr⁻¹	0.110	No significant trend	−6.11	−13.29–1.06	−7.16	Negative tendency, but not statistically significant
Green ET (ET_{green})	km³ yr⁻¹	0.174	No significant trend	−1.61	−4.77–1.55	−1.93	Generally follows rainfall variability
Blue ET (ET_{blue})	km³ yr⁻¹	0.139	No significant trend	5.09	0.69–9.50	3.26	Positive OLS tendency, especially in high-ET_a years
Exploitable water	km³ yr⁻¹	0.124	No significant trend	−1.42	−2.57 to −0.28	−1.04	Statistically significant negative OLS trend
Available water	km³ yr⁻¹	0.124	No significant trend	−1.40	−2.52 to −0.27	−1.06	Statistically significant negative OLS trend

Other basin-scale WA + indicators not shown here are provided in Supplementary Table S4.

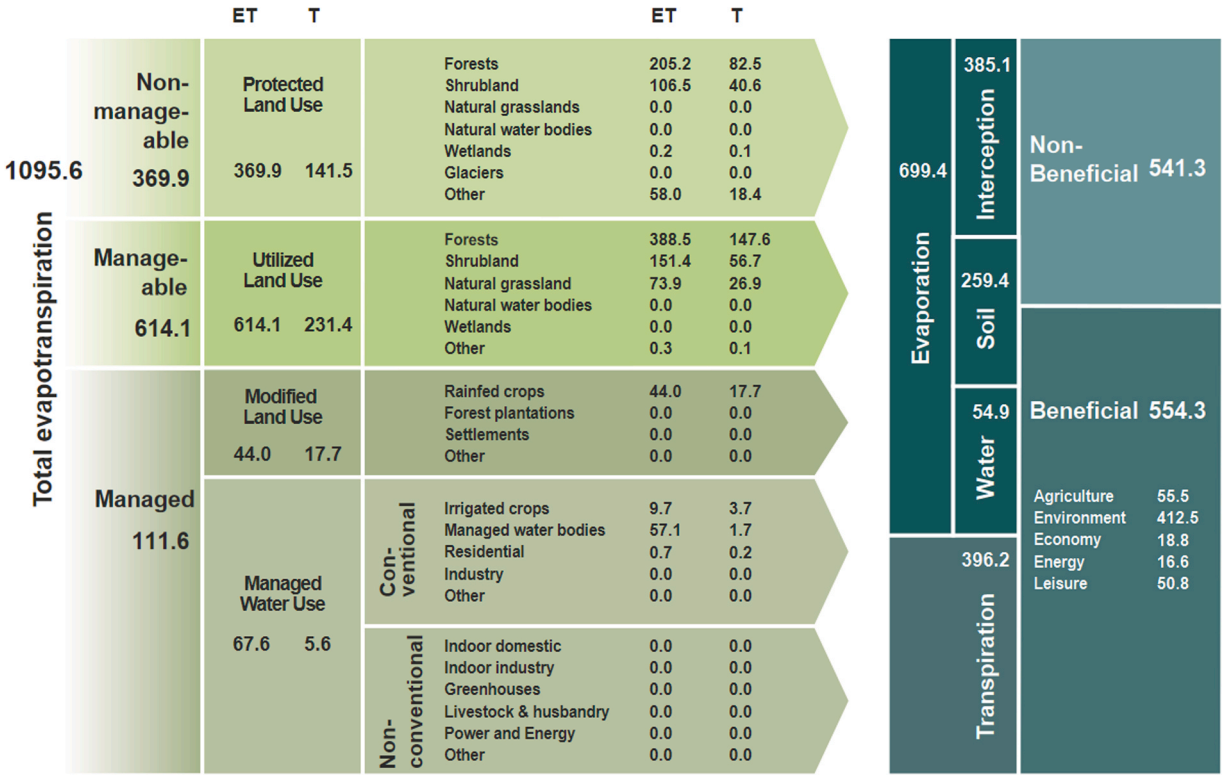


Fig. 7. Average ET sheet for the period 2003–2023.

ecosystems.

Temporally, basin-scale ET components reached their highest values in 2022, followed by a slight decrease in 2023 (Fig. 8). In 2022, *non-manageable ET*, *manageable ET*, and *managed ET* reached 447.7 km³ , 752.4 km³ , and 124.4 km³ , respectively. In 2023, these values declined to 408.4 km³ , 694.3 km³ , and 114.0 km³ , but remained elevated relative to much of the preceding period. A similar pattern was observed for biomass-related ET components. *Transpiration*, *agricultural ET*, and *irrigation ET* peaked in 2022 at 723.4 km³ , 88.2 km³ , and 12.5 km³ , respectively, before declining in 2023–618.2 km³ , 77.0 km³ , and 11.5 km³ . Trend analysis indicates that these recent peaks should be interpreted as high recent values superimposed on mixed long-term tendencies rather than uniform increases across all ET components (Supplementary Table S4). Total *ET*a increased by 3.49 km³ per year, but the trend was not statistically significant. *Non-manageable ET* and *manageable ET* showed positive but non-significant OLS slopes of 1.46 and 1.95 km³ per year, respectively, while *managed ET* remained nearly stable. In contrast, *transpiration* increased significantly, with an OLS slope of 8.22 km³ per year, and *agricultural* ET al.so showed a significant positive OLS trend of 0.74 km³ per year. These results

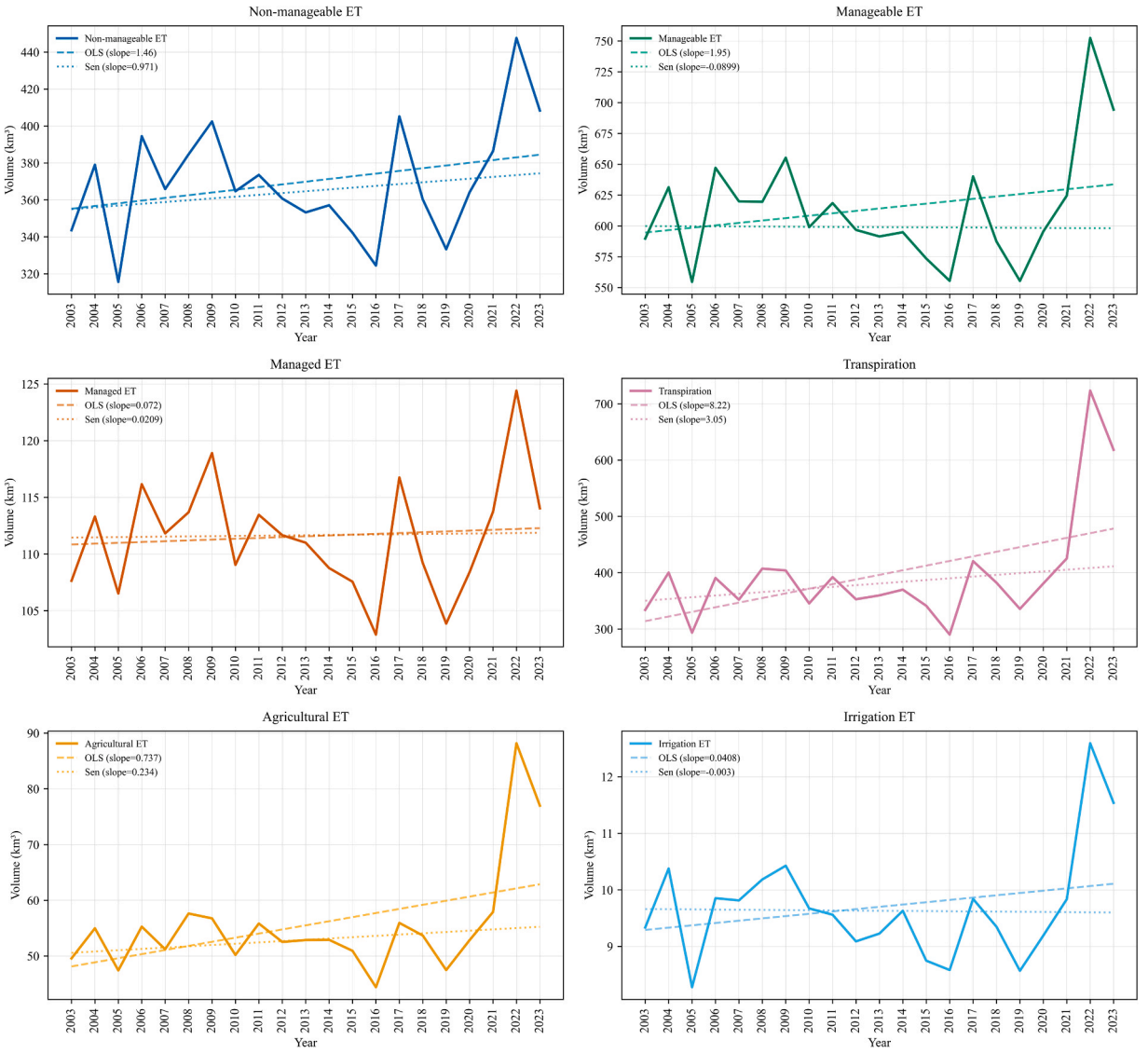


Fig. 8. Inter-annual ET-based water consumption of the ZRB.

Table 5
Average contributions of ZRB sub-basins to water balance components, 2003–2023.

Sub-basin	Area (km^2)	*Precipitation (P)*		*Actual ET (ET_a)*		Surface Water Yield		*Blue ET (ET_{blue})*		*Green ET (ET_{green})*	
		mm	km^3	mm	km^3	mm	km^3	mm	km^3	mm	km^3
Zambezi Delta	11,138.6	936.6	10.4	946.4	10.5	−9.9	−0.1	222.9	2.5	723.6	8.1
Shire	160,446.5	1147.5	184.1	836.6	134.2	310.9	49.9	314.7	50.5	521.9	83.7
Tete	196,637.0	839.8	165.1	642.1	126.3	197.7	38.9	196.6	38.6	445.6	87.6
Mupata	19,010.1	777.7	14.8	816.5	15.5	−38.7	−0.7	281.8	5.4	534.7	10.2
Luangwa	148,974.1	964.5	143.7	770.1	114.7	194.4	29.0	192.0	28.6	578.1	86.1
Kafue	155,996.6	1003.9	156.6	916.8	143.0	87.2	13.6	284.8	44.4	632.0	98.6
Kariba	165,210.8	684.8	113.1	685.4	113.2	−0.7	−0.1	215.6	35.6	469.9	77.6
Cuando	154,761.3	748.3	115.8	712.8	110.3	35.5	5.5	209.1	32.4	503.8	78.0
Luanginga	41,951.7	982.3	41.2	827.7	34.7	154.6	6.5	261.4	11.0	566.3	23.8
Lungwebungo	46,867.0	1069.8	50.1	934.7	43.8	135.1	6.3	284.6	13.3	650.1	30.5
Kabompo	72,274.3	1161.0	83.9	1119.3	80.9	41.7	3.0	313.9	22.7	805.5	58.2
Upper Zambezi	93,434.6	1183.9	110.6	930.5	86.9	253.4	23.7	270.3	25.3	660.2	61.7
Barotse	106,485.9	853.1	90.8	763.9	81.3	89.2	9.5	208.8	22.2	555.2	59.1

indicate a general increase in productive water consumption across the ZRB, particularly through *transpiration*, while the broader ET categories show weaker long-term statistical evidence. The significant decline in *irrigation ET* fraction further indicates that, although absolute *irrigation ET* increased slightly, irrigation accounted for a decreasing share of *agricultural ET* over the study period.

4.3. Sub-catchment contributions

Sub-basin water-balance components varied substantially across the ZRB, reflecting differences in basin area, rainfall intensity, land cover, open-water extent, wetlands, and *ET* losses. As shown in Table 5 and Fig. 9, average annual *P* volumes differed markedly among the 13 sub-basins. The Zambezi Delta recorded the lowest precipitation volume at 10.4 km^3 per year, whereas the adjacent Shire sub-basin contributed the highest at 184.1 km^3 per year. The Tete, Kafue, Luangwa, Cuando, Kariba, and Upper Zambezi sub-basins also each received more than 100 km^3 of *P* annually, contributing 165.1 km^3, 156.6 km^3, 143.7 km^3, 115.8 km^3, 113.1 km^3, and 110.6 km^3 to gross inflow, respectively.

When normalised by area, a different pattern emerged. The Shire sub-basin received 1147.5 mm per year, compared with 936 mm per year in the Zambezi Delta. Despite high *P* volumes, annual rainfall in the Kariba, Cuando, Tete, and Luangwa sub-basins remained below 1000 mm. Their high precipitation volumes, therefore, largely reflect extensive surface area rather than high rainfall intensity. Together, these results confirm strong spatial heterogeneity in hydroclimatic inputs across the ZRB and, consequently, uneven water availability.

Actual ET showed a comparable pattern. The highest ET_a volume was recorded in the Kafue sub-basin, averaging about 143.0 km^3 per year, whereas the highest ET_a intensity occurred in the Kabompo sub-basin at 1119.3 mm per year. The latter is consistent with its high rainfall intensity and substantial forest cover. The lowest ET_a intensity was observed in the Tete sub-basin

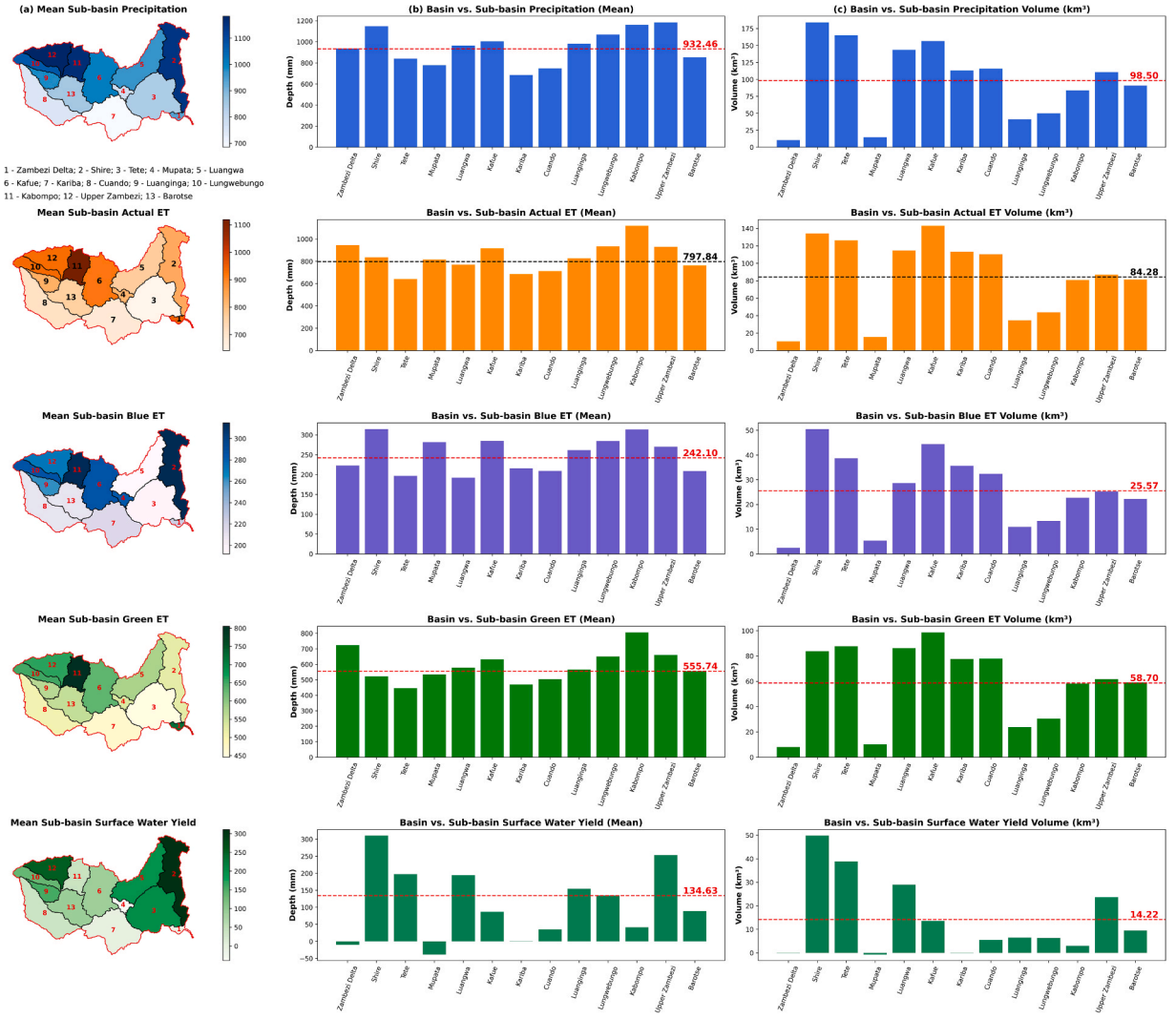


Fig. 9. Average sub-basin water balance components of the ZRB.

(642.1 mm per year), while the lowest ET_a volume occurred in the Zambezi Delta sub-basin (10.5 km³ per year). Overall, the spatial distribution of ET_a broadly followed that of precipitation.

Surface water yield exhibited a similar spatial pattern. The highest yield volumes were recorded in the Shire, Tete, and Luangwa sub-basins, averaging 49.9 km³ , 38.9 km³ , and 29.0 km³ per year, respectively. Despite its relatively high P and large surface area, the Kafue sub-basin generated only 13.6 km³ of surface water per year, reflecting high ET_a losses. The Kariba sub-basin likewise combined high precipitation volume with extensive area but recorded a slightly negative surface water yield (−0.1 km³ per year), again reflecting high ET_a. The lowest surface water yield was observed in the Mupata sub-basin (−0.7 km³ per year). Sub-basins with negative surface water yield function as hydrological sinks, where ET_a losses exceed P inputs, whereas those with positive surface water yield act as net runoff-generating areas, with the surplus contributing to streamflow, storage, or downstream water availability.

The highest ET_{blue} intensities were recorded in the Shire and Kabompo sub-basins, at 314.7 mm and 313.9 mm per year, respectively. In volumetric terms, the Shire sub-basin recorded the highest ET_{blue} in the basin, averaging 50.5 km³ per year, largely because of the presence of Lake Malawi. Other sub-basins with substantial ET_{blue} volumes included the Kafue (44.4 km³), Tete (38.6 km³), Kariba (35.6 km³), and Cuando (32.4 km³). The elevated ET_{blue} in the Kafue sub-basin likely reflects substantial blue-water consumption associated with major wetlands, open-water surfaces, and regulated storage systems, including the Kafue Flats, Lukanga Swamps, and Itezhi-Tezhi reservoir. In the Tete and Kariba sub-basins, the large reservoirs Cahora Bassa and Lake Kariba, respectively, together with economic activity, contribute to high ET_{blue} volumes. In the Cuando sub-basin, elevated ET_{blue} is associated with extensive wetland systems. The lowest ET_{blue} volume was recorded in the Zambezi Delta sub-basin, which, as the smallest sub-basin by area, averaged only 2.5 km³ year.

The Kabompo sub-basin, characterised by substantial forest cover, recorded the highest ET_{green} intensity at 805.5 mm per year. In volumetric terms, the Kafue sub-basin had the highest annual ET_{green}, averaging 98.6 km³ per year. Both sub-basins also receive relatively high P levels, which contribute to their elevated ET_{green} values. The lowest ET_{green} intensity was observed in the Tete sub-basin (445.6 mm per year), while the lowest ET_{green} volume was again recorded in the Zambezi Delta (8.1 km³ year). Across all sub-basins, ET_{green} exceeded ET_{blue}, indicating that rainfall-derived soil moisture is the dominant source of ET_a in the ZRB. However, the relative contributions of ET_{green} and ET_{blue} varied among sub-basins. In the Zambezi Delta, ET_a comprised 24% ET_{blue} and 76% ET_{green}, whereas in the Shire sub-basin, ET_a comprised 38% ET_{blue} and 62% ET_{green}.

As illustrated in Fig. 10, the Luanginga, Lungwebungo, Mupata, and Zambezi Delta sub-basins recorded transpiration volumes well below the sub-basin average of 30.5 km³ yr^{-1} , likely because of their relatively small surface areas. Despite its extensive forest cover, the Kabompo sub-basin also exhibited comparatively low annual transpiration volumes. By contrast, higher transpiration volumes were observed in the Kafue, Kariba, Luangwa, and Tete sub-basins.

4.4. WA + Indicators for the ZRB

Selected WA + indicators were used to translate the basin water-balance components into management-relevant measures of ecological stress, agricultural water use, beneficial depletion, basin closure and per capita water availability. Overall, the indicators show a basin with increasing ecological water stress, declining water availability per person, and rising closure pressure, while agricultural evaporation remained a small fraction of total ET_a. The trend diagnostics for the indicators discussed in this section are

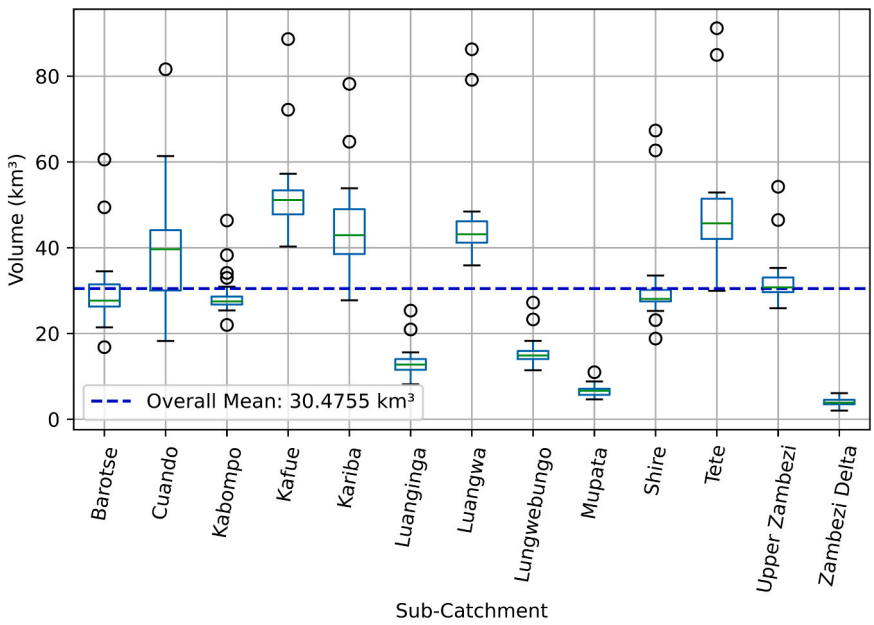


Fig. 10. Box plot of annual average transpiration volumes per sub-basin in the ZRB.

summarised in Table 6, while the full set of basin-scale indicators is provided in Supplementary Table S4.

Environmental Water Stress (EWS), interpreted using the environmental-flow-adjusted water-stress thresholds described in the Methods, averaged 0.53 over 2003–2023, placing the basin in the medium water-stress category on average. Inter-annually, EWS ranged from 0.45 in 2013 (low stress) to 0.79 in 2023 (high stress). Although the Mann–Kendall test did not indicate a statistically significant monotonic trend ($p = 0.124$), the OLS trend was positive and statistically significant, with a slope of 0.0084 per year (95% CI: 0.0025–0.0142). This indicates a gradual increase in ecological pressure on available water resources, with the highest stress occurring in the final year of the analysis.

The Evaporative Stress Index (ESI), which indicates the degree to which ET_a approaches potential ET (ET_p), showed moderate spatial variation across sub-basins. Higher ESI values indicate greater evaporative satisfaction relative to ET_p, while lower values indicate stronger ET limitation. The highest long-term average ESI was observed in the Tete Sub-basin (0.66), followed by Shire (0.64), Cuando (0.63), Barotse (0.62) and Kariba (0.62). In contrast, the lowest ESI values were observed in Kabompo (0.46) and the Zambezi Delta (0.49). These results indicate that evaporative conditions varied across the basin, but without extreme differentiation among sub-basins.

The Agricultural Evaporation Fraction (AEF), representing agricultural ET as a share of total ET_a, remained consistently low over the study period, with a mean of 0.05 and a range of 0.045–0.067. AEF increased slightly in the final years, reaching 0.067 in 2022 and 0.063 in 2023. Both the Mann–Kendall test ($p = 0.037$) and OLS trend (slope = 0.00045 per year; 95% CI: 0.00012–0.00078) indicate a small but statistically significant increase. However, the low magnitude of AEF shows that agricultural ET remained a limited component of total basin ET_a. By comparison, the Beneficial Fraction (BF), representing the share of ET_a attributed to transpiration and therefore biomass production, was substantially higher, averaging 0.36 and ranging from 0.30 in 2016–0.55 in 2022. BF also increased significantly over time, with a Mann–Kendall p-value of 0.009 and an OLS slope of 0.0057 per year (95% CI: 0.0019–0.0095). Together, the AEF and BF results indicate that while agricultural depletion remained small relative to total ET_a, the transpiration component of ET_a increased, particularly in the later years of the study period.

Water Availability Per Capita (WAPC) declined over the study period, indicating increasing pressure on water availability relative to population. WAPC averaged 2880.8 m^3 per person per year, ranging from 3503.5 m^3 per person per year in 2014–1441.7 m^3 per person per year in 2023. Although the Mann–Kendall test did not indicate a significant monotonic trend ($p = 0.124$), the OLS trend was significantly negative, with a slope of −46.5 m^3 per person per year (95% CI: −83.9 to −9.1). Because WAPC is derived from available water and population, this decline reflects the combined effect of population growth and reduced available water, particularly in the final years when available water reached its lowest level.

The Basin Closure Fraction (BCF) averaged 61.7% over the study period and increased from 59.2% in 2003–84.7% in 2023. The highest BCF values occurred in 2022 (81.8%) and 2023 (84.7%), coinciding with years of high ET_a and reduced available water. The Mann–Kendall test did not indicate a significant monotonic trend ($p = 0.110$), but the OLS trend was positive and statistically significant, with a slope of 0.77 %age points yr^{-1} (95% CI: 0.22–1.32). This suggests increasing basin closure pressure, especially in the final years of the analysis.

5. Discussion

5.1. Implications of water balance findings in the Zambezi River Basin

The WA + assessment of the ZRB provides critical insights into the hydrology and water resource status of the region. One prominent finding is the net-positive water balance of the basin: even after current uses, roughly 42 km^3 /year of water remains utilisable outflow on average. This suggests that, at least in aggregate, the ZRB may retain some potential additional capacity for water development without immediately exceeding renewable supplies. Such a surplus can be encouraging for economic development plans. However, the decline in *available water* between 2003 and 2023 raises concerns about the future water security of the basin. Basin-scale trend statistics indicate that *P* showed a downward tendency and ET_a an upward tendency over the study period, but neither trend was statistically significant. By contrast, *exploitable water* and *available water* showed significant negative OLS trends. Taken together, these results suggest that the reduction in available water is more clearly supported statistically than the basin-wide tendencies in *P* and ET_a

Table 6
Trend statistics and descriptive values for WA + indicators, 2003–2023.

Indicator	Mann–Kendall p-value	Mann–Kendall result	OLS slope	95% CI of OLS slope	Sen's slope	Main interpretation
Environmental Water Stress (EWS)	0.124	No significant monotonic trend	0.0084	0.0025–0.0142	0.0059	Medium stress on average, increasing to high stress in 2023
Agricultural Evaporation Fraction (AEF)	0.037	Increasing	0.00045	0.00012–0.00078	0.00019	Agricultural ET remained small but increased slightly
Beneficial Fraction (BF)	0.009	Increasing	0.0057	0.0019–0.0095	0.0029	Beneficial transpiration share increased over time
Basin Closure Fraction (BCF)	0.110	No significant monotonic trend	0.77	0.22–1.32	0.54	Basin closure pressure increased, especially in 2022–2023
Water Availability Per Capita (WAPC)	0.124	No significant monotonic trend	−46.5	−83.9 to −9.1	−35.3	Per capita water availability declined over the study period

alone. However, the analysis suggests that downward tendencies in rainfall, combined with the upward tendency in ET_a, have contributed downward tendencies in total renewable water over time. If these climatic tendencies and trends continue under climate change, the surplus of 42 km^3 could diminish, bringing the basin closer to closure in the coming decades. Hughes and Farinosi (2020) project an increase in *ET* demand across all warming scenarios (1.5°C, 2.0°C, and 3.0°C), accompanied by a dominant drying trend due to climate change. This serves as a cautionary note: current water availability should not foster complacency, and careful planning is essential to ensure water security in the face of drier future scenarios. As of2023, the basin is 85% closed, with a BCF of 0.85.

Another significant implication is the exceptionally high proportion of water depleted through ET_a, which accounts for 94% of net inflow. The results show that the ZRB water balance is primarily driven by ET_a, as it is the dominant mechanism of water loss, supporting Schleiss and Matos' (2017) assertion that the hydrological processes in the ZRB are largely governed by evaporation, despite an annual average rainfall of 1000 mm and above. This effect is especially evident in sub-basins with large open water bodies and wetlands, such as the Shire. In practical terms, only about ~5% of the rainfall contributes to river outflow, as shown in the results, which aligns with the assertion by Schleiss and Matos (2017) that less than 10% of the water discharges into the Indian Ocean. This means the basin is heavily dependent on internal water recycling and green water use. This situation has several consequences: (1) improvements in land management practices, such as soil moisture conservation, afforestation, or wetland restoration, could influence the balance between water depletion and runoff. For example, increased soil evaporation efficiency from agricultural practices or higher transpiration rates from reforestation could further reduce runoff. Conversely, interventions like rainwater harvesting or precision agriculture might reduce non-beneficial ET. (2) The small fraction of outflow also means that downstream riparian countries, such as Mozambique, receive the remainder of an already ET-heavy system, highlighting the importance of upstream-downstream coordination. Any significant increase in upstream consumptive use will directly reduce flows to downstream users and ecosystems, as there is little slack in the outflow. The dominance of ET_a suggests that improving water use efficiency in agriculture, for example by increasing yield per drop, is one of the few feasible ways to create additional usable water.

The positive storage change estimated for the ZRB ($\Delta S \approx 115.9$ km^3 per year) suggests substantial water-storage potential within the basin. However, this estimate applies to the basin as a whole and should not be interpreted as groundwater recharge alone. In the WA + framework, ΔS represents net storage change and may reflect changes in groundwater, soil moisture, surface-water storage, reservoirs, wetlands, and residual uncertainty. Positive values may indicate storage accumulation, including potential recharge, whereas negative values may indicate net depletion or withdrawal. Nevertheless, the magnitude of the estimated positive storage change is broadly consistent with the 130 km^3 /year recharge estimate reported by Senzanje and Dirwai (2020), differing by about 10%. The basin is also known to contain major aquifer systems, including the Kalahari Group sediment aquifers and the Karoo volcanic and sedimentary aquifers (Banda, et al., 2025). For water managers, this highlights the potential value of conjunctive use, combining groundwater and surface water, particularly as a buffer during dry years. Banda et al. (2025) further note that despite numerous perennial rivers in the ZRB, seasonal fluctuations often limit surface-water availability for irrigation during the dry season. In this context, stored water resources could play an important supplementary role. Moreover, increasing demand for irrigation and domestic supply, together with reservoir evaporation losses, is expected to place growing pressure on available water resources (Sainz Sánchez, 2018). This underscores the increasing importance of groundwater and other stored water resources in meeting future water needs. With careful development of groundwater resources and continued monitoring of aquifer levels, drought resilience could be enhanced without significantly affecting river flows, provided that abstraction remains within sustainable limits.

5.2. *Water-food-energy nexus considerations*

The WA + assessment shows that the ZRB exemplifies the water-food-energy-ecosystems nexus, with blue-water depletion concentrated around major reservoirs, wetlands, and managed water-use areas, and with rising environmental water stress signalling increasing trade-offs between hydropower- and irrigation-related water use and ecological flow requirements. A key message from the WA + assessment is that agricultural evapotranspiration remains a relatively small share of total basin ET (AEF ~5%), but this should not be interpreted to mean that irrigation can expand without consequences. In absolute terms, that share still represents roughly 50–60 km^3 of ET, while the basin as a whole is already strongly ET-dominated and has high basin closure. This means that any further increase in consumptive water use must be evaluated not only in terms of agricultural expansion, but also against likely gains in food production, implications for hydropower reliability, reservoir storage demands, environmental flow requirements, and climate risk.

Despite this level of agricultural water consumption, basin-wide agricultural output remains modest, as agriculture is still dominated by rainfed systems and irrigated areas remain limited (Senzanje and Dirwai, 2020; Joint Research Centre, 2021). This suggests a potential water productivity gap, but confirming this would require additional analysis linking agricultural ET to crop yield or biomass production information. Particularly in the MLU areas (rainfed farmlands), *ET* is much lower than in natural vegetation zones due to water stress, and yields are also low, indicating an opportunity to improve rainfed agriculture to better utilise the available green water. Meanwhile, in MWU zones such as irrigated sugar or maize schemes, water productivity (kg of crop per m^3 of ET) could be enhanced through improved irrigation scheduling and technologies, since any water not transpired productively is essentially lost as non-beneficial evaporation. For instance, the transition to drip irrigation from furrow or sprinkler systems enhances the WEFE nexus performance of irrigated agriculture across different agro-climatic regions, optimising water, energy, and land use efficiency under a changing climate to bring about inclusive and sustainable development across the globe (Taguta et al., 2022). Policies promoting efficient irrigation techniques and crop choices with high water productivity can yield more food while using the same amount of water. Furthermore, the water security prospects of the region should prioritise climate-smart strategies, such as managed aquifer recharge (MAR), to maintain water availability, even during extreme drought conditions (Banda et al., 2024).

The high ET_{blue} values in reservoirs and lake-dominated sub-basins show that open-water evaporation is a major consumptive

component of the basin's energy and water storage infrastructure. In dry years, this evaporative loss can significantly deplete live storage, reducing firm power output. There is a trade-off in the nexus: increasing reservoir capacity for energy or multi-year storage inherently increases evaporative surface area. Thus, future energy planning might consider complementary investments in solar or other renewables to reduce the need for additional large reservoirs. This is crucial for the ZRB, where hydropower output potential is projected to decrease under a medium emission scenario: −9% in the 2020 s, −18% in the 2050 s, and −28% in the 2080 s, driven by reduced inflows and increased evaporation (Hamududu and Killingtveit, 2016). Additionally, investments in alternative energy sources result in the maintenance of environmental flows downstream (captured in the reserved outflow using the EWR), which are crucial to the sustainability of fisheries and ecosystem services that indirectly support both food production and livelihoods.

5.3. Climate change and resilience

Climate-change and water-use scenarios indicate that impacts vary substantially across the ZRB (Hughes and Farinosi, 2020). The strongest effects are expected in areas containing large natural and man-made surface water bodies, which are particularly vulnerable to increasing aridity.

A critical concern for the ZRB is the growing drought risk and increasing evaporative demand, both of which may exacerbate runoff reductions (Hamududu and Killingtveit, 2016). This analysis, which highlights recent storage depletion, suggests that the basin has been drawing on its savings to meet demand during dry periods. Continued reliance on storage drawdown would become increasingly risky and unsustainable if droughts become longer, more frequent, or more intense. Banda and Shilengwe (2025) used the Standard Precipitation Evapotranspiration Index (SPEI) to detect severe droughts that occurred in 1991/92, 1994/95, 1997/98, 2001/02, 2004/05, 2011/12, 2015/16, and 2018/19, likely impacting groundwater storage in the Upper Zambezi. Their analysis found that 3-month SPEI correlated with GRACE groundwater storage anomaly data, with an R^2 of ~0.5, which was an indication of a short-term response to drought conditions. Banda and Shilengwe (2025) proposed three key interventions to enhance groundwater climate resilience: MAR, groundwater banking during wet years, and establishing local groundwater reserves. To build climate resilience, strategies should include augmenting storage to capture wet-year surpluses for use in dry years, enhancing the use of seasonal forecasts to proactively manage reservoir releases and water allocations, and protecting or improving natural infrastructure, such as wetlands and forests, that regulates hydrology, offering flood mitigation and water release during droughts. A positive finding is the substantial storage recharge observed, suggesting that in wet years, a portion of water infiltrates aquifers, ensuring future access. Policy frameworks should promote MAR and the conservation of recharge zones to maintain groundwater as a reliable drought reserve. Additionally, small-scale water harvesting and soil and water conservation initiatives at the community level can bolster local agricultural resilience in the face of increasingly erratic rainfall patterns.

The EWS index, which has been rising toward 80% in recent years, is a warning sign for ecological resilience. It indicates high environmental-flow stress and suggests that during droughts, river flows at key ecological nodes may be insufficient to meet the needs of aquatic ecosystems. This can lead to habitat degradation and long-term ecological shifts, such as encroachment of terrestrial vegetation into drying wetlands (European Commission, 2015; Miller et al., 2013). To avoid such outcomes, it will be vital to enforce environmental flow allocations even when competing demands increase. This might involve difficult trade-offs during drought, but the long-term sustainability of the natural capital of the basin depends on it.

5.4. Comparison with other WA + applications

Recent WA + applications place the ZRB in a useful comparative context. Relative to the Volta Basin, the ZRB has a higher average basin closure of 62%, but greater remaining utilisable water. Owusu et al. (2025) report an average basin closure of 55% and about 20 km^3 per year of utilisable water for the Volta, indicating some scope for further allocation but also clear pressure from existing consumption. By contrast, the ZRB results indicate a more ET-dominated but still only partially allocated system, with current utilised flow of 44.4 km^3 per year and 42.0 km^3 per year remaining as utilisable outflow. Both studies nevertheless point to the importance of spatially uneven water availability and the need for transboundary cooperation when interpreting basin-scale surpluses.

The Lake Tana sub-basin study by Mekonnen et al. (2026) offers a more recent and methodologically comparable example of how WA + indicators can be linked directly to allocation and environmental-flow concerns. Their study frames water availability per capita (WAPC), environmental water stress (EWS), basin closure, and beneficial fraction (BF) as policy-relevant indicators and shows how WA + can be used to assess trade-offs among irrigation, hydropower, and downstream ecological flows. This is closely aligned with the present ZRB assessment, where rising EWS, substantial ET_{blue} over reservoirs and wetlands, and marked sub-basin contrasts in water yield all point to increasing competition between productive water use and ecological requirements

A comparison with the Volta climate-change WA + study by Dembélé et al. (2023) is also instructive. That study reported a very high BCF (0.93) for the Volta under baseline conditions, indicating that a large fraction of basin inflow is already consumed and/or stored. In contrast, the ZRB remains less constrained at the basin scale, although the present results also show that pressure is far from negligible, especially where ET_{blue} is concentrated and where EWS has risen. Taken together, these comparisons suggest that the ZRB is not yet in the category of the most tightly closed basins, but neither is it a basin in which additional development can be assumed to be consequence-free. Rather, the WA + results indicate a basin in which future development must be carefully assessed against sub-basin variability, seasonal availability, hydropower reliability, reservoir evaporation, and ecological flow needs.

The older Indus Basin WA + application (Karimi et al., 2013b) is a useful foundational benchmark because it demonstrated the value of spatially explicit accounting in a highly managed transboundary system. However, unlike the Indus, the ZRB is still dominated by rainfall-supported ET and retains a measurable volume of unallocated outflow. The main message from the present comparison is

therefore not that the ZRB resembles a fully closed irrigation basin, but that WA + reveals where development pressures are already intensifying and where basin-scale averages may mask important local constraints. This study thus provides a contemporary baseline against which future changes in closure, environmental stress, and water-use allocation can be tracked.

Selected comparisons with recent WA + applications are summarised in Table 7.

5.5. Limitations

Uncertainty in the precipitation (*P*) forcing remains an important limitation despite the basin-wide rainfall product evaluation undertaken in this study. CHIRPS performed strongly relative to the other tested products and was retained because it combined high correlation, low bias, strong hydrological efficiency metrics and finer spatial resolution than MSWEP. Nevertheless, *P* estimates remain dependent on the spatial distribution and quality of station observations used for validation, and rainfall uncertainty can propagate into ET, runoff, exploitable water and water-scarcity indicators.

Actual ET (ET_a) was based on SSEBop v6.1, which is suitable for large-scale basin assessment and has been supported by previous applications and evaluations across Africa. However, ET was not directly validated against basin-wide flux-tower or lysimeter observations because such observations are not readily available at the ZRB scale. The ET results should therefore be interpreted as remotely sensed estimates subject to product uncertainty, particularly over heterogeneous miombo woodland, wetlands, irrigated areas, open-water systems and seasonally water-stressed landscapes.

The LULC component was also subject to temporal uncertainty because ESA CCI annual maps were available only up to 2020 at the time of the original WA + analysis. The 2020 LULC layer was therefore carried forward for 2021–2023. Supplementary stability checks using ESA CCI-derived LUWA, ESRI/Impact Observatory, Dynamic World and FAOSTAT statistics supported the reasonableness of this assumption at the basin scale. However, the carry-forward approach may not fully capture localised land-cover changes during 2021–2023, and this uncertainty may affect class-based allocation, ET partitioning and land-use-dependent WA + indicators.

Discharge validation was limited by the lack of consistent long-term observed discharge records across the basin and at sub-basin outlets. The GRDC-based reconstructed outlet discharge series provided an independent constraint on mean-flow plausibility, with low validation-period bias, but showed limited ability to reproduce detailed daily flow variability. Consequently, the discharge assessment was used as an outlet-level uncertainty check for runoff and surface-water outflow components, rather than as a direct validation of each annual WA + water-balance term.

5.6. Policy recommendations

The findings of this study carry several important implications for water management and policy in the ZRB. The WA + findings suggest several policy priorities for sustainable and equitable water management in the ZRB.:

(a) *Improve Agricultural Water Productivity Rather than Expand Consumptive Use*: Improve water use efficiency in agriculture through modern irrigation techniques and better agronomic practices. By adopting irrigation technologies and promoting drought-tolerant crop varieties that reduce non-beneficial evaporation and increase crop production per unit of water consumed. This is important because agricultural ET represents a relatively small share of total basin ETa, suggesting that food production gains should come primarily from improving crop water productivity rather than simply increasing consumptive water use.

(b) *Invest in Climate-Resilient Infrastructure*: Develop and upgrade water infrastructure to buffer against climate variability and change. Coupled with this, strengthen flood management infrastructure and drought contingency plans to handle more extreme hydrological events. Investments should be evaluated for evaporative efficiency, ensuring that the benefits (hydropower, irrigation) justify the water lost to evaporation.

(c) *Leverage Groundwater Sustainably*: Integrate groundwater use into the water supply strategy of the basin. Given the substantial recharge indicated by the water accounts, groundwater may provide an important buffer in dry years and a source for decentralised water supply. Policies should promote conjunctive use of surface and groundwater. For instance, allow sustainable groundwater abstraction during droughts when river flows are low, and encourage recharge during wet years. Establish basin-wide groundwater monitoring and governance to prevent over-extraction and ensure aquifers are replenished.

(d) *Safeguard Environmental Flows*: Enforce and formalise environmental flow requirements in water allocation plans and dam operations. As water development progresses, it is critical to maintain sufficient flows for the ecosystems of the Zambezi that millions of people also depend on. We recommend that the ZAMCOM and member states adopt clear environmental flow targets for critical river reaches and integrate these into dam release schedules and abstraction permits. During drought conditions, minimum environmental flows thresholds should be protected in allocation policies, alongside essential human needs to avoid irreversible ecological damage.

(e) *Strengthen Transboundary Coordination and Data Sharing*: Building on the ZAMCOM framework, enhance the harmonisation of water laws and data exchange among the eight riparian countries. A basin-wide water allocation plan that accounts for upstream and downstream needs should be developed, including the additional ~42 km^3 of utilisable outflow identified in this study, which should be allocated carefully to maximise regional benefits while preventing unilateral over-exploitation. Regular sharing of data will improve trust and enable coordinated responses to floods and droughts. We also recommend institutionalising the WA + accounting process (or similar) on an annual or biennial basis by ZAMCOM, so that all countries have a common, transparent view of the water status in the basin to inform policy decisions.

Table 7
Selected comparisons between the ZRB and other recent WA + applications.

Study	Scale/period	Selected comparable findings	Relevance to the ZRB discussion
Zambezi River Basin (this study)	Basin-wide, 2003–2023	Utilised flow 44.4 km^3 per year; utilisable outflow 42.0 km^3 per year; mean EWS 0.53, rising to 0.79 in 2023; AEF about 0.05	Indicates a basin that remains only partly allocated at the basin scale, but with rising ecological pressure and strong spatial contrasts
Volta Basin (Owusu, et al., 2025)	Basin-wide / sub-basin / country, 2003–2021	Average basin closure 55%; utilisable water about 20 km^3 per year; nearly 25% of exploitable water non-recoverable	Shows a partially open but already pressured transboundary basin where spatial scale matters for interpretation
Lake Tana sub-basin (Mekonnen, et al., 2026)	Sub-basin, 2010–2020	Green ET 68% of total consumption; blue ET 32%; water availability per capita exceeds 1700 m^3 per person per year threshold	Demonstrates how recent WA + applications connect basin indicators directly to allocation and environmental-flow management
Volta Basin under climate change (Dembélé, et al., 2023)	Basin-wide modelling, baseline 1991–2020 and future	Basin closure 0.93	Useful contrast showing a much more tightly constrained basin, reinforcing that the ZRB still has room for development, but not without trade-offs
Indus Basin (Karimi et al., 2013b)	Basin-wide	Highly managed, irrigation-dominated transboundary basin	A foundational WA + benchmark for comparison of governance and spatially explicit allocation, not as the closest recent analogue

Overall, these comparisons suggest that the ZRB remains less constrained than some heavily allocated WA + basins, but that future development decisions must still be evaluated against ecological flow needs, storage losses, and strong spatial variability in water availability.

Implementing these recommendations will help ensure that the water resources of the ZRB are developed sustainably and equitably, balancing economic growth with ecosystem preservation. By proactively planning under the guidance of scientific assessments like WA + , policymakers and water managers can improve the resilience of the basin to climate variability, meet the growing water demands, and uphold the commitments of regional agreements and the Sustainable Development Goals related to water.

6. Conclusion

This study demonstrated the application of the WA + framework to the transboundary ZRB, yielding a comprehensive picture of water availability, consumption, and distribution for 2003–2023. The WA + results reveal a complex and evolving water balance: Although the basin receives substantial amounts of precipitation, much of this input is depleted through ETa, and precipitation is unevenly distributed across sub-basins, leaving a much smaller fraction as river outflow, and utilisable water. Nonetheless, the basin currently maintains a positive water balance, with significant volumes of water remaining available for further utilisation. We found that approximately 86.4 km^3 of water is available for use each year, of which only about half is currently being used. These results indicate that development may still be possible in selected locations and seasons, but only under careful allocation planning that accounts for environmental flows, downstream users, climate risk, and consumptive water losses. Not all sub-basins have surplus water, and notably, total available water has exhibited a downward tendency in recent years due to a downward tendency in rainfall. Our analysis underscores the importance of IWRM: improvements in water use efficiency, careful allocation among sectors, and adaptive strategies for climate resilience are all necessary to secure the water future of the basin. The WA + framework proved a valuable decision-support tool in this context, enabling us to assess the ZRB despite limited ground data. By utilising satellite observations, WA + provided spatially consistent estimates of key water balance components such as ET_{green} and ET_{blue}, which are difficult to quantify using ground observations alone. The insights gained, such as the magnitude of consumptive use in certain sub-basins or the estimation of groundwater recharge, offer a scientific basis for policy actions. We encourage basin authorities and researchers to continue and refine this accounting regularly, possibly integrating more recent remote sensing advances. In closing, the ZRB stands at a juncture where informed management can harness its considerable water resources for development while avoiding the pitfalls of over-exploitation. By following the recommendations outlined and strengthening cooperation under frameworks like ZAMCOM, the riparian nations can ensure that such coordinated monitoring and planning will be essential to balance water resources development, ecological protection, and climate resilience in the ZRB. The application of WA + here serves as a model for other data-scarce basins seeking to achieve sustainable water management through innovative tools and collaborative governance.

Authors' contributions

Micheal Katongo Phiri conceived the ideas, implemented the methodology and developed the manuscript; Kawawa Banda provided supervision and review of manuscript, methodology and fund raising. Naga Velpuri and Mansoor Leh provided supervision and review of the manuscript. Primrose Tinonetsana gap-filled the Zambezi outlet discharge. All authors contributed critically to the drafts and gave final approval for publication.

CRediT authorship contribution statement

Micheal Katongo Phiri: Writing – original draft, Visualization, Methodology, Data curation, Conceptualization. **Kawawa Banda:** Writing – review & editing, Supervision, Funding acquisition. **Mansoor Leh:** Writing – review & editing, Supervision, Methodology.

Naga Velpuri: Writing – review & editing, Supervision, Methodology. **Primrose Tinonetsana:** Data curation.

Funding

This work is funded through the WARFSA Fellowship offered through NEPAD SANWATCE coordinated by Stellenbosch University. Partial support was received from the ACEWATER III Project and WaterNET.

Declaration of Competing Interest

The authors declare that they have no known competing financial interests or personal relationships that could have appeared to influence the work reported in this paper.

Acknowledgements

Special thanks to IWMI Sri Lanka for hosting me and allowing me to gain critical skills to perform WA + analysis, and from providing the processing platform for the analysis.

Appendix A. Supporting information

Supplementary data associated with this article can be found in the online version at doi:10.1016/j.ejrh.2026.103692.

Data availability

Data will be made available on request.

References

Akpoti, K., Velpuri, N.M., Leh, M., Kagone, S., Mekonnen, K., Owusu, A., Senay, G.B., 2026. VegET evapotranspiration for Africa: continental-scale simulation, multi-product evaluation, and drought assessment. J. Hydrol. Reg. Stud. 66, 103511. https://doi.org/10.1016/j.ejrh.2026.103511.

Anderson, M.C., Zolin, C.A., Sentelhas, P.C., Hain, C.R., Semmens, K., Yilmaz, M.T., Tetrault, R., 2016. The evaporative stress index as an indicator of agricultural drought in Brazil: an assessment based on crop yield impacts. Remote. Sens. Environ. 174, 82–89. https://doi.org/10.1016/j.rse.2015.11.034.

Bamweyana, I., Musinguzi, M., Kayondo, L.M., 2021. Evaluation of CHIRPS satellite gridded dataset as an alternative rainfall estimate for localized modelling over Uganda. Atmos. Clim. Sci. 11, 797–811. https://doi.org/10.4236/acs.2021.114046.

Banda, K., Crestaz, E., Seliger, R., Mengistu, H., Sauramba, J., Saraiva, M., 2025. Zambezi River Basin aquifer systems: opportunities and challenges in using freely available data sources and groundwater flow modelling for spatial exploratory analysis. Groundw. Sustain. Dev. 29, 101421. https://doi.org/10.1016/j.gsd.2025.101421.

Banda, K., Phiri, M.K., Nyambe, I., 2024. Response of remote sensing-based climatic indicators to drought conditions during El Niño events and implications for water–food–energy nexus. Water Pract. Technol. 19 (9), 3439–3453. https://doi.org/10.2166/wpt.2024.232.

Banda, K., Shilengwe, C., 2025. Identifying potential hotspots of groundwater-climate interaction in the Kalahari Aquifer System, Upper Zambezi Basin, Southern Africa. J. Hydrol. Reg. Stud. 60, 102484. https://doi.org/10.1016/j.ejrh.2025.102484.

Bastiaanssen, W.G. 2009. Water accountants: De nieuwe generatie waterbeheercontroleurs, intreerede (in Dutch). Delft: Delft University of Technology, Department of Civil Engineering and Geosciences.

Bastiaanssen, W., Ha, L.T., & Fenn, M. (2015). Water Accounting Plus (WA+) for Reporting Water Resources Conditions and Management: A Case Study in the Ca River Basin, Vietnam. Arlington: Winrock International.

Batchelor, C., Hoogeveen, J., Faurès, J.-M., Peiser, L., 2016. Water Accounting and Auditing - A Sourcebook. Food and Agriculture Organization of the United Nations, Rome.

Beilfuss, R., 2012. A Risky Climate for Southern African Hydro: Assessing Hydrological Risks and Consequences for Zambezi River Basin Dams. International Rivers, Berkeley.

Brown, C.F., Brumby, S.P., Guzder-Williams, B., Birch, T., Hyde, B.S., Mazzariello, J., Tait, A.M., 2022. Dynamic world, near real-time global 10m land use land cover mapping. Sci. Data 9, 251. https://doi.org/10.1038/s41597-022-01307-4.

Dembélé, M., Salvadore, E., Zwart, S., Ceperley, N., Grégoire, M., Bettina, S., 2023. Water accounting under climate change in the transboundary Volta River Basin with a spatially calibrated hydrological model. J. Hydrol. 626, 130092. https://doi.org/10.1016/j.jhydrol.2023.130092.

ESA. 2017. Land Cover CCI Product User Guide Version 2. Tech. Rep. Retrieved November 22, 2024, from maps.elie.ucl.ac.be/CCI/viewer/download/ESACCI-LC-Ph2-PUGv2_2.0.pdf.

ESRI & Impact Observatory. 2026. Sentinel-2 10 m land use/land cover time series. Retrieved from ArcGIS Living Atlas of the World: ⟨https://livingatlas.arcgis.com/en/home/⟩.

European Commission. 2015. Ecological flows in the implementation of the Water Framework Directive (Guidance Document No. 31). Luxembourg: Publications Office of the European Union. doi:10.2779/775712.

Falkenmark, M., Rockström, J., 2006. The NEw Blue and Green Water Paradigm: Breaking New Ground for Water Resources Planning and Management. J. Water Resour. Plan. Manag. 132 (3), 129–132. https://doi.org/10.1061/(ASCE)0733-9496(2006)132:3(129).

FAO. 1997. Irrigation potential in Africa: A basin approach. Rome: Food and Agriculture Organization of the United Nations.

FAO. 2012. Coping with water scarcity: An action framework for agriculture and food security. Rome: Food and Agriculture Organization of the United Nations.

FAO. 2024. SDG indicator metadata: Indicator 6.4.2—Level of water stress: Freshwater withdrawal as a proportion of available freshwater resources (Harmonized metadata template, version 1.1). Food and Agriculture Organization of the United Nations (FAO).

FAO. 2024. Global Map of Irrigation Areas (GMIA). Retrieved March 18, 2024, from ⟨https://www.fao.org/land-water/land/land-governance/land-resources-planning-toolbox/category/details/en/c/1029519/⟩.

FAO. 2026. FAOSTAT: Land Cover. Rome: Food and Agriculture Organization of the United Nations.

Funk, C., Peterson, P., Landsfeld, M., Pedreros, D., Vardin, J., Shukla, S., Michaelsen, J., 2015. The climate hazards infrared precipitation with stations—a new environmental record for monitoring extremes. Sci. Data 2 (1), 150066. https://doi.org/10.1038/sdata.2015.66.
Hamududu, B.H., Killingtveit, Å., 2016. Hydropower production in future climate scenarios; the case for the Zambezi River. Energies 9 (7), 502. https://doi.org/10.3390/en9070502.
Hughes, D.A., Farinosi, F., 2020. Assessing development and climate variability impacts on water resources in the Zambezi River basin. Simulating future scenarios of climate and development. J. Hydrol. Reg. Stud. 32, 100763. https://doi.org/10.1016/j.ejrh.2020.100763.
Hulsman, P., Savenije, H.H., Hrachowitz, M., 2021. Satellite-based drought analysis in the Zambezi River Basin: Was the 2019 drought the most extreme in several decades as locally perceived? J. Hydrol. Reg. Stud. 34, 100789. https://doi.org/10.1016/j.ejrh.2021.100789.
Joint Research Centre. 2021. WEFE nexus in Africa (JRC Technical Report). Ispra: Publications Office of the European Union.
Karimi, P., Bastiaanssen, W., 2015. Spatial evapotranspiration, rainfall and land use data in water accounting – Part 1: review of the accuracy of the remote sensing data. Hydrol. Earth Syst. Sci. 19 (1), 507–532. https://doi.org/10.5194/hess-19-507-2015.
Karimi, P., Bastiaanssen, W., Molden, D., 2013a. Water Accounting Plus (WA+)–a water accounting procedure for complex river basins based on satellite measurements. Hydrol. Earth Syst. Sci. 17 (7), 2459–2472. https://doi.org/10.5194/hess-17-2459-2013.
Karimi, P., Bastiaanssen, W., Molden, D., Cheema, M., 2013b. Basin-wide water accounting based on remote sensing data: an application for the Indus Basin. Hydrol. Earth Syst. Sci. 17 (7), 2473–2486. https://doi.org/10.5194/hess-17-2473-2013.
Karimi, P., Bastiaanssen, W., Sood, A., Hoogeveen, J., Peiser, L., Bastidas-Obando, E., Dost, R.J., 2015. Spatial evapotranspiration, rainfall and land use data in water accounting – Part 2: reliability of water acounting results for policy decisions in the Awash Basin. Hydrol. Earth Syst. Sci. 19 (1), 533–550. https://doi.org/10.5194/hess-19-533-2015.
Karimi, P., Pareeth, S., Michailovsky, C., 2019. Rapid assessment of the water accounts in Urmia Lake basin. Project report. IHE Delft Institute for Water Education. Delft: IHE Delft Institute for Water Education. Retrieved from ⟨https://www.wateraccounting.org/files/projects/urmia/Urmia_Projecct_Phase1_Final_Report.pdf⟩.
Lehner, B., Grill, G., 2013. Global river hydrography and network routing: baseline data and new approaches to study the world's large river systems. Hydrol. Process. 27 (15), 2171–2186. https://doi.org/10.1002/hyp.9740.
Lehner, B., Reidy Liermann, C., Revenga, C., Vörösmarty, C., Fekete, B., Crouzet, P., Wisser, D., 2011. High-resolution mapping of the world's reservoirs and dams for sustainable river-flow management. Front. Ecol. Environ. 9 (9), 494–502. https://doi.org/10.1890/100125.
Lehner, B., Verdin, K., Jarvis, A., 2008. New global hydrography derivedfrom spaceborne elevation data. March 4 Eos Trans. Am. Geophys. Union. 89 (10), 93–104.
Liu, C., Kroeze, C., Hoekstra, A.Y., Gerbens-Leenes, W., 2012. Past and future trends in grey water footprints of anthropogenic nitrogen and phosphorus inputs to major world rivers. Ecol. Indic. 18, 42–49. https://doi.org/10.1016/j.ecolind.2011.10.005.
Martens, B., Miralles, D.G., Lievens, H., van der Schalie, R., de Jeu, R.A., Fernández-Prieto, D., Verhoest, N.E., 2017. GLEAM v3: satellite-based land evaporation and root-zone soil moisture. May 1y Geosci. Model. Dev. 10 (5), 1903–1925. https://doi.org/10.5194/gmd-10-1903-2017.
Mekonnen, K., Velpuri, N.M., Leh, M., Akpoti, K., Owusu, A., Tinonetsana, P., Munzimi, Y., 2023. Accuracy of satellite and reanalysis rainfall estimates over Africa: a multi-scale assessment of eight products for continental applications. J. Hydrol. Reg. Stud. 49, 101514. https://doi.org/10.1016/j.ejrh.2023.101514.
Mekonnen, K., Velpuri, N.M., Leh, M., Akpoti, K., Owusu, A., Mahapatra, S., Seid, A., 2026. An integrated modeling framework for water accounting assessment in the Lake Tana Sub-Basin, Ethiopia: impacts of interbasin water transfer. J. Hydrol. Reg. Stud. 65, 103318. https://doi.org/10.1016/j.ejrh.2026.103318.
Miller, K.A., Webb, J.A., de Little, S.C., Stewardson, M.J., 2013. Environmental flows can reduce the encroachment of terrestrial vegetation into river channels: a systematic literature review. Environ. Manag. 52 (5), 1202–1212. https://doi.org/10.1007/s00267-013-0147-0.
Miralles, D.G., Holmes, T.R., de Jeu, R.A., Gash, J.H., Gash, J.H., Meesters, A.G., Dolman, A.J., 2011. Global land-surface evaporation estimated from satellite-based observations. Hydrol. Earth Syst. Sci. 15 (2), 453–469. https://doi.org/10.5194/hess-15-453-2011.
Myneni, R.B., Hoffman, S., Knyazikhin, Y., Privette, J.L., Glassy, J., Tian, Y., Running, S.W., 2002. Global products of vegetation leaf area and fraction absorbed PAR from year one of MODIS data. Remote. Sens. Environ. 83 (1–2), 214–231. https://doi.org/10.1016/S0034-4257(02)00074-3.
Myneni, R., Knyazikhin, Y., Park, T., 2015. MOD15A2H MODIS/Terra Leaf Area Index/FPAR 8-Day L4 Global 500m SIN Grid V006. Sioux Falls, South Dakota, USA: NASA EOSDIS Land Processes Distributed Active Archive Center. doi:10.5067/MODIS/MOD15A2H.006.
Ndhlovu, G., Woyessa, Y., 2021. Evaluation of streamflow under climate change in the zambezi river basin of Southern Africa. Water 13 (21), 3114. https://doi.org/10.3390/w13213114.
Owusu, A., Akpoti, K., Leh, M., Perera, T., Madushanka, L., Mekonnen, K., Velpur, N.M., 2025. Bridging scales and borders on water availability and use in the transboundary Volta River Basin: a water accounting approach. J. Hydrol. Reg. Stud. 59, 102377. https://doi.org/10.1016/j.ejrh.2025.102377.
Patle, P., Singh, P.K., Rakkasagi, S., Ahmad, I., Goyal, M.K., 2023. Application of water accounting plus framework for the assessment of the water consumption pattern and food security. In: Gupta, A.K., Goyal, M.K., Singh, S.P. (Eds.), Ecosystem Restoration: Towards Sustainability and Resilient Development. Disaster Resilience and Green Growth. Springer, Singapore, Singapore, pp. 257–269. https://doi.org/10.1007/978-981-99-3687-8_14.
Republic of Botswana. 2016. Botswana water accounting report 2014/15. Ministry of Minerals, Energy and Water Resources, Department of Water Affairs. Gaborone: World Bank.
Republic of Zambia. 2020. Natural capital accounts for water, 2010–2016: first results and next steps. Ministry of Water Development, Sanitation and Environmental Protection and Ministry of National Development Planning, Department of Water Resources Development. Lusaka: World Bank.
Running, S.W., Mu, Q., Zhao, M., 2015. MOD17A2H MODIS/Terra Gross Primary Productivity 8-Day L4 Global 500 m SIN Grid V006. Sioux Falls, South Dakota, USA: NASA EOSDIS Land Processes Distributed Active Archive Center. doi:10.5067/MODIS/MOD17A2H.006.
Running, S.W., Nemani, R.R., Heinsch, F.A., Zhao, M., Reeves, M., Hashimoto, H., 2004. A continuous satellite-derived measure of global terrestrial primary production. BioScience 54 (6), 547–560. https://doi.org/10.1641/0006-3568(2004)054[0547:ACSMOG]2.0.CO;2.
Running, S.W., Zhao, M., 2019. MOD17A3HGF MODIS/Terra Net Primary Production Gap-Filled Yearly L4 Global 500 m SIN Grid V006. Sioux Falls, South Dakota, USA: NASA EOSDIS Land Processes Distributed Active Archive Center. doi:10.5067/MODIS/MOD17A3HGF.006.
Sainz Sánchez, G., 2018. The Zambezi River Basin: Water Resources Management: Energy-Food-Water Nexus Approach. Master's thesis. Stockholm University, Department of Physical Geography, Stockholm. Retrieved from. ⟨https://www.diva-portal.org/smash/get/diva2:1244639/FULLTEXT01.pdf⟩.
Schleiss, A.J., Matos, J.P., 2017. Zambezi River Basin. In: Singh, V.P. (Ed.), Handbook of Applied Hydrology, 2nd ed. McGraw-Hill Education, New York, New York, USA, pp. 98-1–98-7. Retrieved from. https://infoscience.epfl.ch/handle/20.500.14299/132466.
Senay, G.B., Bohms, S., Singh, R.K., Gowda, P.H., Velpuri, N.M., Alemu, H., Verdin, J.P., 2013. Operational EVapotranspiration Mapping Using Remote Sensing and Weather Datasets: A New Parameterization For the SSEB approach. J. Am. Water Resour. Assoc. (JAWRA) 49 (3), 577–591. https://doi.org/10.1111/jawr.12057.
Senzanje, A., Dirwai, T.L., 2020. Water and Agriculture in the Zambezi River Basin: Characterization of Current Agriculture Activities, Future Potential Irrigation Developments and Food Security to Face Climate Variability in the Zambezi River Basin. University of KwaZulu-Natal, Bioresources Engineering Programme and Centre for Water Resources Research. University of KwaZulu-Natal, Pietermaritzburg. Retrieved from. https://aquaknow.jrc.ec.europa.eu/system/files/Annex30_Senzanjie_UnKWZN_FinalReport.pdf?utm_source=chatgpt.com.
Simons, G., Koster, R., Droogers, P., 2020. HiHydroSoil v2.0 – High Resolution Soil Maps of Global Hydraulic Properties. July 8. FutureWater B.V, Wageningen.
Smakhtin, V.U., Revenga, C., Döll, P., 2004. A pilot global assessment of environmental water requirements and scarcity. Water Int. 29 (3), 307–317. https://doi.org/10.1080/02508060408691785.
Taguta, C., Dirwai, T.L., Senzanje, A., Sikka, A., Mabhaudhi, T., 2022. Sustainable irrigation technologies: a water-energy-food (WEF) nexus perspective towards achieving more crop per drop per joule per hectare. Environ. Res. Lett. 17 (7), 073003. https://doi.org/10.1088/1748-9326/ac7b39.
Tinonetsana, P., Leh, M., Mekonnen, K., Akpoti, K., Owusu, A., & Velpuri, N. n.d. (unpublished results). Strengthening African Hydrological Data Through Reanalysis and Gap Filling of the GRDC Discharge Database for Selected River Basins in Africa.
United Nations. (2012). System of environmental-economic accounting for water. New York: United Nations, Department of Economic and Social Affairs, Statistics Division. Retrieved from ⟨https://unstats.un.org/unsd/publication/seriesf/Seriesf_100e.pdf?utm_source=chatgpt.com⟩.
Velpuri, N.M., Senay, G.B., 2017. Partitioning Evapotranspiration into Green and Blue Water Sources in the Conterminous United States. Sci. Rep. 7 (1), 6191. https://doi.org/10.1038/s41598-017-06359-w.

WDPA. (2023). World database on protected areas. Retrieved October 10, 2023, from ⟨https://www.protectedplanet.net/en/thematic-areas/wdpa?tab=WDPA⟩.
Weerasinghe, I., Bastiaanssen, W., Mul, M., Jia, L., van Griensven, A., 2020. Can we trust remote sensing evapotranspiration products over Africa? Hydrol. Earth Syst. Sci. 24 (3), 1565–1586. https://doi.org/10.5194/hess-24-1565-2020.
World Bank. (2010). The Zambezi River Basin - a multi-sector investment opportunities analysis (Vol. 3). Washingtone D.C: World Bank.
Zimba, H., Coenders-Gerrits, M., Banda, K., Schilperoort, B., van de Giesen, N., Nyambe, I., Savenije, H.H., 2023. Phenophase-based comparison of field observations to satellite-based actual evaporation estimates of a natural woodland: miombo woodland, southern Africa. Hydrol. Earth Syst. Sci. 27 (8), 1695–1722. https://doi.org/10.5194/hess-27-1695-2023.